Available online at www.sciencedirect.com
ScienceDirect
Journal of Sound and Vibration 309 (2008) 129–149
JOURNAL OF SOUND AND VIBRATION
www.elsevier.com/locate/jsvi

Existence and analytical predictions of periodic motions in a periodically forced, nonlinear friction oscillator

Albert C.J. Luo*, Patrick Zwiegart Jr.

Department of Mechanical and Industrial Engineering, Southern Illinois University Edwardsville, Edwardsville, IL 62026-1805, USA

Received 1 August 2005; received in revised form 22 September 2006; accepted 7 June 2007
Available online 14 September 2007

Abstract

The grazing bifurcation, stick phenomena and periodic motions in a periodically forced, nonlinear friction oscillator are investigated. The nonlinear friction force is approximated by a piecewise linear, kinetic friction model with the static force. The total forces for the input and output flows to the separation boundary are introduced, and the force criteria for the onset and vanishing of stick motions are developed through such input and output flow forces. The periodic motions of such an oscillator are predicted analytically through the corresponding mapping structure. Illustrations of the periodic motions in such a piecewise friction model are given for a better understanding of the stick motion with the static friction. The force responses are presented, which agreed very well with the force criteria. If the fully nonlinear friction force is modeled by several portions of piecewise linear functions, the periodically forced, nonlinear friction oscillator can be predicted more accurately. However, for the fully nonlinear friction force model, only the numerical investigation can be carried out.

1. Introduction

The force criteria of the stick and non-stick flows for the harmonically driven linear oscillator with dry-friction were developed recently in Luo and Gegg [1,2]. For such an oscillator, the periodic motions were predicted analytically through the appropriate mapping structures, and the stick and non-stick flows were observed. Furthermore, Luo and Gegg [3,4] used the non-smooth theory of Luo [5] to systematically investigate the mechanism of grazing and stick flows in such a friction oscillator. The sufficient and necessary conditions were obtained for the existence of the grazing and stick flows to the separation boundary. In that model, the kinetic friction is independent of the velocity except for the friction switching at the zero relative velocity. However, the kinetic friction force in engineering is often a nonlinear function strongly dependent on the relative velocity, and the maximum static friction force is also different from the kinetic friction at the zero velocity. Such a difference causes the vector field of the dynamical system to have the flow barrier. The flow barriers of the vector fields in discontinuous dynamical systems were systematically discussed in Luo [6]. The flow barriers existing in the vector fields of dynamical systems will lead to more difficulty to investigate such

*Corresponding author. Tel.: +1 618 650 5389; fax: +1 618 650 2555.
E-mail address: aluo@siue.edu (A.C.J. Luo).

0022-460X/$ - see front matter © 2007 Elsevier Ltd. All rights reserved.
doi:10.1016/j.jsv.2007.06.067

dynamical systems. Therefore, a periodically forced oscillator with a piecewise linear friction model is investigated, and the jump from the maximum static friction to kinetic friction is also considered. The objective of this investigation is to demonstrate how to develop the appropriate methodology and criteria for discontinuous dynamical systems with flow barriers. To avoid computational errors, the nonlinear kinetic friction force is modeled by a piecewise linear friction instead of the full nonlinear model in this paper. That is because the oscillator with the full nonlinear friction model can only be solved numerically, in which case it is very difficult to verify the analytical criteria. A mathematical discussion of the problem follows.

Consider a dynamical system with nonlinear friction, but the nonlinear friction is approximated by a piecewise linear model, as shown in Fig. 1. The dynamical system consists of a mass (m), a spring of stiffness (k) and a damper of viscous damping coefficient (r). The oscillator mass rests on the horizontal belt surface traveling with a constant speed (V). The coordinate system (x, t) is absolute with displacement x and time t. The periodic excitation force $Q_0 \cos \Omega t$ exerts on the mass, where Q_0 and Ω are the excitation strength and frequency, respectively. The piecewise linear friction force is given by

$$\bar{F}_f(\dot{x}) \begin{cases} = \mu_1(\dot{x} - V_1) - \mu_2(V_1 - V) + F_N\mu_k, & \dot{x} \in [V_1, \infty), \\ = -\mu_2(\dot{x} - V) + F_N\mu_k, & \dot{x} \in (V, V_1), \\ \in \left[-\mu_s F_N, \mu_s F_N\right], & \dot{x} = V, \\ = -\mu_3(\dot{x} - V) - F_N\mu_k, & \dot{x} \in (V_2, V), \\ = \mu_4(\dot{x} - V_2) - \mu_3(V_2 - V) - F_N\mu_k, & \dot{x} \in (-\infty, V_2], \end{cases} \tag{1}$$

where $\dot{x} \triangleq \mathrm{d}x/\mathrm{d}t$. μ_s, μ_k and F_N are static and kinetic friction coefficients and a normal force to the contact surface, respectively. The coefficients μ_j ($j = 1, 2, 3, 4$) are the slopes for friction force with velocity. For this problem, $F_N = mg$ and g is the gravitational acceleration. In fact, this model can be applied to many mechanical problems, and the normal force can be exerted externally.

If the mass sticks on the belt surface, the total non-friction force per unit mass, acting on the mass in the x-direction, is determined by

$$F_{\mathrm{nf}} = A_0 \cos \Omega t - 2\,\mathrm{d}V - cx \quad \text{for } \dot{x} = V, \tag{2}$$

where $A_0 = Q_0/m$, $d = r/2m$ and $c = k/m$. For the stick motion, the non-friction force is less than the maximum static friction force, i.e.,$|F_{\mathrm{nf}}| \leqslant F_{f_s}$ and $F_{f_s} = \mu_s F_N/m$. The mass does not have any relative motion to the belt. Therefore, no acceleration exists because the belt speed is constant, i.e.,

$$\ddot{x} = 0 \quad \text{for } \dot{x} = V. \tag{3}$$

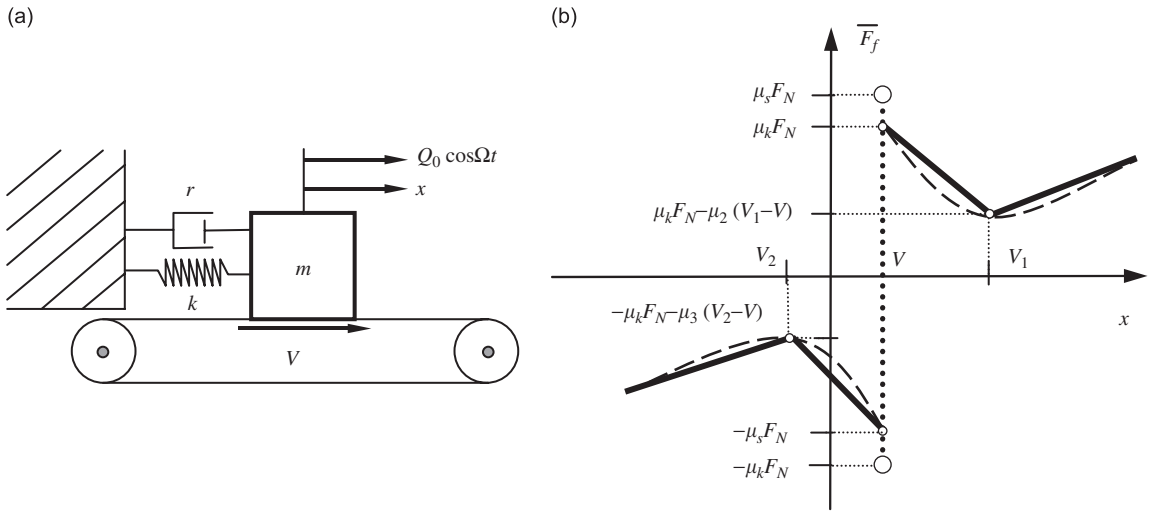

Fig. 1. (a) Schematic mechanical model of the friction-induced oscillator and (b) piecewise linear friction force model.

Once the stick motion exists already, if the non-friction force is greater than the maximum static friction force on the mass (i.e., $|F_{\rm nf}| > F_{f_s}$), the stick motion disappears. If any stick motion does not exist before, the total force acting on the mass for the non-stick motion is

$$F = A_0 \cos \Omega t - F_{f_k} - 2\,\mathrm{d}\dot{x} - cx \quad \text{for } \dot{x} \neq V, \tag{4}$$

where $F_{f_k} = \bar{F}_f/m$ for $\dot{x} \neq V$. Therefore, the equation of non-stick motion for this dynamical system with a piecewise linear friction is

$$\ddot{x} + 2\,\mathrm{d}\dot{x} + cx = A_0 \cos \Omega t - F_{f_k} \quad \text{for } \dot{x} \neq V. \tag{5}$$

The above model is used to investigate the dynamics behavior of the periodically forced, nonlinear friction oscillator. Such a problem is of great interest in engineering because friction-induced oscillations extensively exist in engineering. For a long period, many researchers have paid a great attention on this problem. However, this problem has not been solved yet owing to the discontinuity.

In 1931, Den Hartog [7] focused only on the non-stick periodic motion of the periodically forced linear oscillator with Coulomb and viscous damping. In 1960, Levitan [8] discussed a friction oscillation model with the base driven periodically, and the stability of the non-stick, periodic motion was discussed through the Poincare mapping concept. Based on the Coulomb friction oscillator, in 1964, Filippov [9] developed a theory for differential equations with discontinuous right-hand sides. The concept of differential inclusion was introduced via the set-valued analysis, and the existence and uniqueness of the solution for such a discontinuous differential equation were discussed. The comprehensive discussion of such discontinuous differential equations can be referred to Ref. [10]. The Filippov's theory mainly focused on the existence, uniqueness and stability of the solutions for non-smooth dynamical systems. However, Luo [5] investigated the local singularity in the vicinity of the separation boundary, and the certain criteria were developed to determine the local singularity and sliding motions on the discontinuous boundary. Furthermore, the imaginary, sink and source flows were introduced in Ref. [11] to determine the sink and source motions in non-smooth dynamical systems.

In 1979, Hundal [12] estimated the dynamical responses of the base driven friction oscillator. In 1986, Shaw [13] investigated the stability and bifurcation of such a periodic motion through the Poincare mapping. In 1992, Feeny [14] analytically and graphically investigated the non-smoothness of the Coulomb friction oscillator and the regions for stick motion were presented. In 1994, Feeny and Moon [15] gave the experimental and numerical investigations on chaos in a dry-friction oscillator. In 1996, Feeny [16] comprehensively discussed the nonlinear dynamics of oscillators with stick–slip friction. In 1997, Hinrichs, Oestreich and Poop [17] considered the impact and friction involved in the oscillator (also see [18]). The stick and non-stick motions in such an impact and friction oscillator were observed, and chaotic motions were observed through a nonlinear friction model. In 1998, Natsiavas [19] developed an algorithm to determine the periodic motions in piecewise linear oscillators with viscous and dry friction damping, and the stability of such periodic motions was investigated through the perturbation of the initial conditions. Leine et al. [20] presented the limit cycles of the nonlinear friction model through the shooting method. In 1999, Virgin and Begley [21] investigated the grazing bifurcation and attraction basin of an impact-friction oscillator through the interpolated cell mapping method. For a better understanding of friction-induced vibration, one tried to develop the approximate solutions of responses in friction-induced oscillation. In 2001, Ko et al. [22] investigated the fiction-induced vibrations with and without external excitations. In 2002, Andreaus and Casini [23] considered a friction-impact model with Coulomb friction without external excitation; and the closed-form solutions were presented. In 2003, Thomsen and Fidlin [24] presented the approximate, analytical amplitude for the free stick–slip vibration with a nonlinear friction model. Kim and Perkins [25] used the harmonic balance/Galerkin method to investigate non-smooth stick–slip oscillator. In 2004, Pilipchuk and Tan [26] investigated the friction-induced vibration of a two-degree-of-freedom mass–damper–spring system interacting with a decelerating rigid strip. Li and Feng [27] investigated the bifurcation and chaos in the friction-induced oscillator with a nonlinear friction model.

To investigate non-smooth dynamical systems, the mapping techniques have been extensively used. For instance, the mapping concepts have been adopted to determine the periodic motion in impacting systems (e.g., [28–30]). This methodology was also employed to investigate the periodic and chaotic motions of the periodically driven piecewise linear systems in Refs. [31,32]. A generalized methodology was given in Ref. [33] for complicated periodic motions in such a piecewise linear system. To determine the unsteady process in

machines, in 1994, Pfeiffer [34] considered both the impacts and frictions existing in the oscillator. Furthermore, in 1996, Glocker and Pfeiffer [35] developed the theory for multibody dynamics with unilateral contacts to solve such a complicated dynamics in machines. In 1999, Pfeiffer [36] gave a brief survey of the theory of the unilateral multibody dynamics, and presented some typical applications for ones to refer (also see [37]). In addition, the discontinuous map was developed at the discontinuous boundary to investigate the complex dynamics of non-smooth dynamical systems (e.g., [38–40]), and the corresponding normal forms were also developed at the discontinuous boundary.

In this paper, the piecewise linear, kinetic friction model with static friction will be used to approximate the nonlinear friction forces in the periodically driven friction oscillator. The non-smooth dynamical theory in Ref. [5] will be used to develop the conditions for the grazing bifurcation, and the onset and vanishing of stick motions in such a friction oscillator. Because the jump between the static and kinetic friction exists, the input and output flow forces will be introduced. The force criteria for the onset and vanishing of stick motions will be developed through the input and output flow forces, and the condition for the grazing bifurcation to the separation boundary will be presented. The mapping techniques will also be used to determine periodic motions of the friction model in Eq. (5). The parameter map for periodic motions in such a friction-induced vibration system will be obtained. Illustrations of the periodic motions in such a piecewise friction model will be given to verify the analytical conditions.

2. Grazing and stick conditions

The discontinuities of this dynamical system are caused by the piecewise linear friction law. Further, the phase plane must be partitioned into four domains. The jump between the static and kinetic friction forces is as a main discontinuity. Therefore, the naming of the phase domains starts from the domain near the main discontinuous boundary for $\dot{x} > V$. Based on the direction of trajectories of mass motion, the corresponding boundaries are named, as shown in Fig. 2. The domain naming can be arbitrarily. The four regions are expressed by Ω_j ($j = 1, 2, \ldots, 4$). In phase plane, the flow and the corresponding vector field for such a system are introduced as

$$\mathbf{x} \triangleq (x, \dot{x})^{\mathrm{T}} \equiv (x, y)^{\mathrm{T}} \quad \text{and} \quad \mathbf{F} \triangleq (y, F)^{\mathrm{T}}. \tag{6}$$

The named domains and the oriented boundaries are expressed by

$$\begin{aligned} \Omega_1 &= \{(x, y) | y \in (V, V_1)\}, \quad \Omega_2 = \{(x, y) | y \in (V_1, \infty)\}, \\ \Omega_3 &= \{(x, y) | y \in (V_2, V)\}, \quad \Omega_4 = \{(x, y) | y \in (-\infty, V_2)\}, \end{aligned} \tag{7}$$

$$\partial\Omega_{ij} = \{(x, y) | \varphi_{ij}(x, y) \equiv y - V_\rho = 0\}, \tag{8}$$

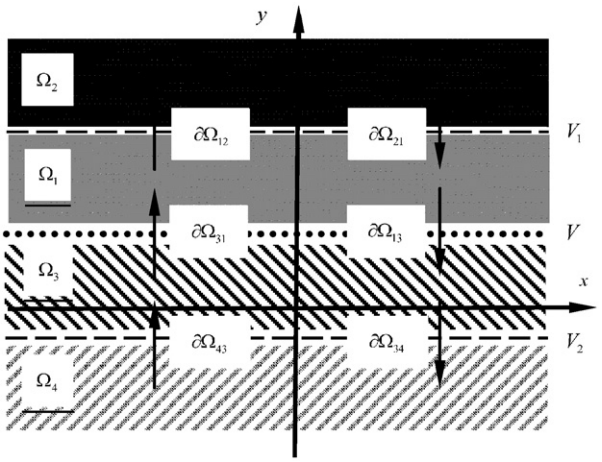

Fig. 2. Phase plane partition and oriented boundaries.

where $\rho = 1$ if $i,j \in \{1,2\}$, $\rho = \varnothing$ if $i,j \in \{1,3\}$ and $\rho = 2$ if $i,j \in \{3,4\}$. The symbol $\varnothing$ represents the empty set. The subscript $(\cdot)_{ij}$ defines the boundary between Ω_i and Ω_j. The domains are accessible for a certain vector field. On the boundary $\partial\Omega_{13}$ or $\partial\Omega_{31}$, the vector fields are discontinuous, but on the boundaries $\partial\Omega_{12}$ and $\partial\Omega_{34}$, the vector fields are C^0-continuous. Based on the definitions of the boundaries and domains in phase space, the equations of motion in Eqs. (3) and (5) are described as

$$\dot{\mathbf{x}} = \mathbf{F}^{(j)}(\mathbf{x}, t), j \in \{0,1,2,3,4\}, \tag{9}$$

where

$$\left.\begin{aligned} &\mathbf{F}^{(0)}(\mathbf{x}, t) = (V, 0)^{\mathrm{T}} \text{ on } \partial\Omega_{13} \text{ or } \partial\Omega_{31}, \\ &\mathbf{F}^{(j)}(\mathbf{x}, t) = \big(y, F_j(\mathbf{x}, t)\big)^{\mathrm{T}} \text{ in } \Omega_j, \ (j \in \{1,2,3,4\}), \\ &F_j(\mathbf{x}, t) = A_0 \cos \Omega t - F_{f_k}^{(j)}(\mathbf{x}, t) - 2d_j y - c_j x. \end{aligned}\right\} \tag{10}$$

The corresponding dynamical friction forces are given by

$$\begin{aligned} F_{f_k}^{(2)}(\mathbf{x}, t) &= \frac{1}{m}\left[\mu_1(\dot{x} - V_1) - \mu_2(V_1 - V) + F_N\mu_k\right], \quad \dot{x} \in [V_1, \infty), \\ F_{f_k}^{(1)}(\mathbf{x}, t) &= -\frac{1}{m}\left[\mu_2(\dot{x} - V) - F_N\mu_k\right], \quad \dot{x} \in (V, V_1), \\ F_{f_k}^{(3)}(\mathbf{x}, t) &= -\frac{1}{m}\left[\mu_3(\dot{x} - V) + F_N\mu_k\right], \quad \dot{x} \in (V_2, V), \\ F_{f_k}^{(4)}(\mathbf{x}, t) &= \frac{1}{m}\left[\mu_4(\dot{x} - V_2) - \mu_3(V_2 - V) - F_N\mu_k\right], \quad \dot{x} \in (-\infty, V_2]. \end{aligned} \tag{11}$$

The two force boundaries relative to $V_{1,2}$ (i.e., $\dot{x} = V_1$ or V_2) are C^0-continuous. However, the boundary relative to the velocity V is a discontinuous force boundary. From the non-smooth dynamical system theory in Luo [5], only on the discontinuous force boundary, the stick motion for $\mathbf{n}_{\partial\Omega_{\alpha\beta}}$ pointing to Ω_α is guaranteed by

$$\left[\mathbf{n}_{\partial\Omega_{\alpha\beta}}^{\mathrm{T}} \cdot \mathbf{F}^{(\alpha)}(\mathbf{x}_m, t_{m-})\right] < 0 \quad \text{and} \quad \left[\mathbf{n}_{\partial\Omega_{\alpha\beta}}^{\mathrm{T}} \cdot \mathbf{F}^{(\beta)}(\mathbf{x}_m, t_{m-})\right] > 0, \tag{12}$$

where $\{\alpha, \beta\} \in \{1, 3\}$ and $\alpha \neq \beta$ with

$$\mathbf{n}_{\partial\Omega_{\alpha\beta}} = \nabla\varphi_{\alpha\beta} = \left(\frac{\partial\varphi_{\alpha\beta}}{\partial x}, \frac{\partial\varphi_{\alpha\beta}}{\partial y}\right)^{\mathrm{T}}_{(x_m, y_m)}. \tag{13}$$

Note that $\nabla = \partial/\partial x\mathbf{i} + \partial/\partial y\mathbf{j}$ is the Hamilton operator. The time t_m represents the moment for the motion just on the separation boundary, and the time $t_{m\pm} = t_m \pm 0$ reflects the flows in the regions instead of the separation boundary. However, the corresponding necessary and sufficient conditions for the non-stick motion (or passable motion) are for $\mathbf{n}_{\partial\Omega_{\alpha\beta}}$ pointing to Ω_α:

$$\begin{aligned} &\left[\mathbf{n}_{\partial\Omega_{\alpha\beta}}^{\mathrm{T}} \cdot \mathbf{F}^{(\alpha)}(\mathbf{x}_m, t_{m-})\right] < 0 \quad \text{and} \quad \left[\mathbf{n}_{\partial\Omega_{\alpha\beta}}^{\mathrm{T}} \cdot \mathbf{F}^{(\beta)}(\mathbf{x}_m, t_{m+})\right] < 0 \quad \text{for} \quad \Omega_\alpha \to \Omega_\beta, \\ &\left[\mathbf{n}_{\partial\Omega_{\beta\alpha}}^{\mathrm{T}} \cdot \mathbf{F}^{(\beta)}(\mathbf{x}_m, t_{m-})\right] > 0 \quad \text{and} \quad \left[\mathbf{n}_{\partial\Omega_{\beta\alpha}}^{\mathrm{T}} \cdot \mathbf{F}^{(\alpha)}(\mathbf{x}_m, t_{m+})\right] > 0 \quad \text{for} \quad \Omega_\beta \to \Omega_\alpha. \end{aligned} \tag{14}$$

Using Eq. (8), Eq. (13) gives for $i, j \in \{1, 2, 3, 4\}$:

$$\mathbf{n}_{\partial\Omega_{ij}} = \mathbf{n}_{\partial\Omega_{ji}} = (0, 1)^{\mathrm{T}}. \tag{15}$$

The normal directions of the boundaries ($\partial\Omega_{12}$ and $\partial\Omega_{21}$), ($\partial\Omega_{13}$ and $\partial\Omega_{31}$) and ($\partial\Omega_{34}$ and $\partial\Omega_{43}$) point to Ω_2, Ω_1 and Ω_3, respectively. Therefore, we have

$$\mathbf{n}_{\partial\Omega_{ji}}^{\mathrm{T}} \cdot \mathbf{F}^{(j)}(t) = \mathbf{n}_{\partial\Omega_{ij}}^{\mathrm{T}} \cdot \mathbf{F}^{(j)}(t) = F_j(\mathbf{x}, t). \tag{16}$$

With Eq. (16), the conditions for stick and non-stick motions in Eqs. (12) and (14) become

$$\begin{aligned}
&\mathbf{F}_1(\mathbf{x}_m, t_{m-}) < 0 \quad \text{and} \quad \mathbf{F}_3(\mathbf{x}_m, t_{m-}) > 0 \quad \text{on} \quad \partial\Omega_{13},\\
&\mathbf{F}_1(\mathbf{x}_m, t_{m-}) < 0 \quad \text{and} \quad \mathbf{F}_3(\mathbf{x}_m, t_{m+}) < 0 \quad \text{for} \quad \Omega_1 \to \Omega_3,\\
&\mathbf{F}_1(\mathbf{x}_m, t_{m+}) > 0 \quad \text{and} \quad \mathbf{F}_3(\mathbf{x}_m, t_{m-}) > 0 \quad \text{for} \quad \Omega_3 \to \Omega_1.
\end{aligned} \tag{17}$$

When the non-stick motion on the boundary $\partial\Omega_{13}$ disappears, the sliding motion on the boundary will be formed. The transition from the non-stick motion to the stick motion on the boundary is called the onset of the stick motion. The detailed discussion of the onset of the stick motion can be referenced to Refs. [4,5]. Therefore, the onset condition for the stick motion is

$$\begin{aligned}
&\mathbf{F}_1(\mathbf{x}_m, t_{m-}) < 0 \quad \text{and} \quad \mathbf{F}_3(\mathbf{x}_m, t_{m+}) = 0 \quad \text{for} \quad \Omega_1 \to \partial\Omega_{13},\\
&\mathbf{F}_3(\mathbf{x}_m, t_{m-}) > 0 \quad \text{and} \quad \mathbf{F}_1(\mathbf{x}_m, t_{m+}) = 0 \quad \text{for} \quad \Omega_3 \to \partial\Omega_{13}.
\end{aligned} \tag{18}$$

Once the stick motion is formed on the boundary $\partial\Omega_{13}$, with varying time or system parameters, the stick motion on the boundary $\partial\Omega_{13}$ will disappear, which is termed the vanishing of the stick motion on the boundary. The theory for non-smooth dynamical systems in Luo [5] gives the force conditions for vanishing of the stick motions, i.e.,

$$\begin{aligned}
&\mathbf{F}_1(\mathbf{x}_m, t_{m-}) < 0 \quad \text{and} \quad \mathbf{F}_3(\mathbf{x}_m, t_{m-}) = 0 \quad \text{for} \quad \partial\Omega_{13} \to \Omega_3,\\
&\mathbf{F}_3(\mathbf{x}_m, t_{m-}) > 0 \quad \text{and} \quad \mathbf{F}_1(\mathbf{x}_m, t_{m-}) = 0 \quad \text{for} \quad \partial\Omega_{13} \to \Omega_1.
\end{aligned} \tag{19}$$

Based on the above conditions, the stick motion on the boundary $\partial\Omega_{13}$ is sketched in Fig. 3. The conditions for the stick motion are depicted through the two vector fields $\mathbf{F}^{(1)}(t)$ and $\mathbf{F}^{(3)}(t)$ in the domains Ω_1 and Ω_3. Because the stick motion is only possible on the boundary $\partial\Omega_{13}$, in the vicinity of such a boundary, the vector fields in two domains are depicted in Fig. 3. In Fig. 3(a), once the trajectory arrives to the boundary, if the normal vector fields on both sides of the separation boundary satisfy the condition in Eq. (12), the flow (or stick motion) will slide on the boundary. With varying time, the condition in Eq. (12) may not be satisfied by the normal vector fields. The sliding flow will disappear. The disappearance condition in Eq. (19) requires that one of the two normal components of the vector fields be zero (i.e., $F_1(t_{m-}) = 0$ or $F_3(t_{m-}) = 0$). In Fig. 3(a), the vanishing of the stick (or sliding) motion with $F_3(t_{m-}) = 0$ is sketched. When the flow from Ω_1 arrives to the discontinuous boundary $\partial\Omega_{13}$, if the first equation of Eq. (17) holds, then the sliding motion will be formed, which is also sketched in Fig. 3(a). Under the conditions in Eq. (18), the flow may slide along the separation boundary, or the flow may pass through the separation boundary. This critical situation is called the sliding or stick motion bifurcation. The detailed discussion was given (e.g., [4,5,11]). For this situation, with varying time or parameters, the stick motion is formed on the boundary. The condition in Eq. (12) should be satisfied to keep the sliding motion. Once the first equation of Eq. (19) is satisfied, the sliding motion will disappear and get into one of the two domains Ω_1 and Ω_3. Such a sliding motion is sketched in Fig. 3(b).

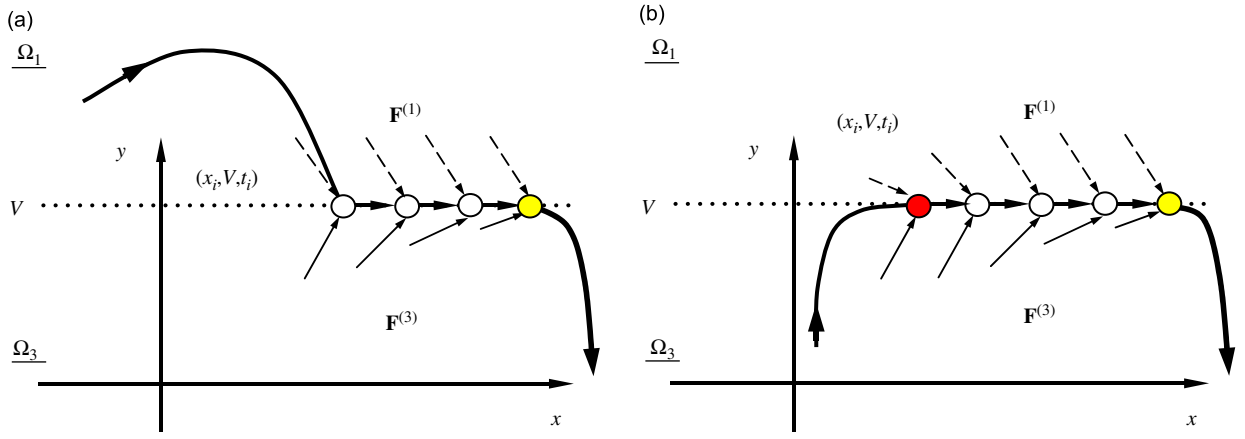

Fig. 3. Vector field for stick motion: (a) vanishing only and (b) onset and vanishing.

From the foregoing discussion, the switching conditions in Eqs. (18) and (19) give four possible sliding motions (I)–(IV), as shown in Fig. 4. The switching conditions given in Eq. (18) are critical for formation of the sliding motion. From Eq. (18), the onset condition has four possible cases, sketched in Fig. 5. The sliding motion starting $(\mathbf{x}_i,\ t_i)$ and vanishing at $(\mathbf{x}_{i+1},\ t_{i+1})$ possess the four cases: $F_3(t_i) = F_3(t_{i+1}) = 0$ (case I), $F_3(t_i) = F_1(t_{i+1}) = 0$ (case II), $F_1(t_i) = F_3(t_{i+1}) = 0$ (case III) and $F_1(t_i) = F_1(t_{i+1}) = 0$ (case IV). The onset conditions of the sliding motion for cases I and IV are the same as for the grazing motion, as discussed latter. The two onsets of the sliding motions can be called the grazing onsets. The other onset conditions based on the cases II and III are the *inflexed* onsets for the sliding motions. The detailed mathematical description can be referred to Luo [5].

The grazing conditions are sketched in Fig. 6 for a constant, switching velocity V. The vector fields $\mathbf{F}^{(i)}(\mathbf{x},\ t)$ and $\mathbf{F}^{(j)}(\mathbf{x},\ t)$ in Ω_i and Ω_j are expressed by the dashed and solid arrow-lines, respectively. In addition to $F_\alpha(\mathbf{x}_m, t_{m\pm}) = 0$ $(\alpha \in \{i,\ j\})$, the sufficient condition for grazing motions on the boundary requires $F_i(\mathbf{x}_m, \Omega t_{m-\varepsilon}) < 0$ and $F_i(\mathbf{x}_m, \Omega t_{m+\varepsilon}) > 0$ in domain Ω_i; and $F_j(\mathbf{x}_m, \Omega t_{m-\varepsilon}) < 0$ and $F_j(\mathbf{x}_m, \Omega t_{m+\varepsilon}) > 0$ in domain Ω_j.

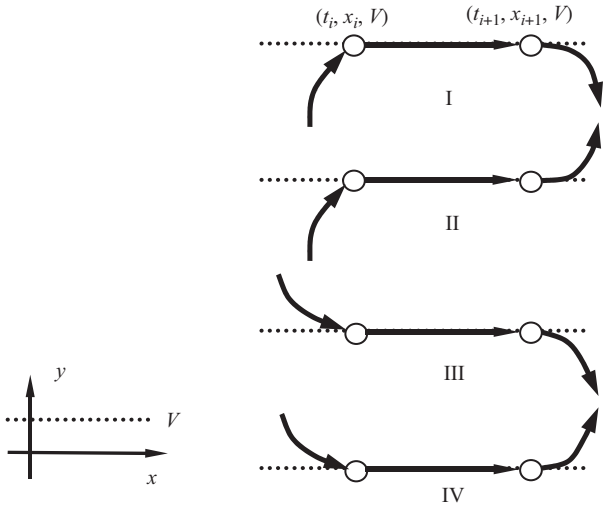

Fig. 4. Classification of sliding motions for belt speed $V > 0$.

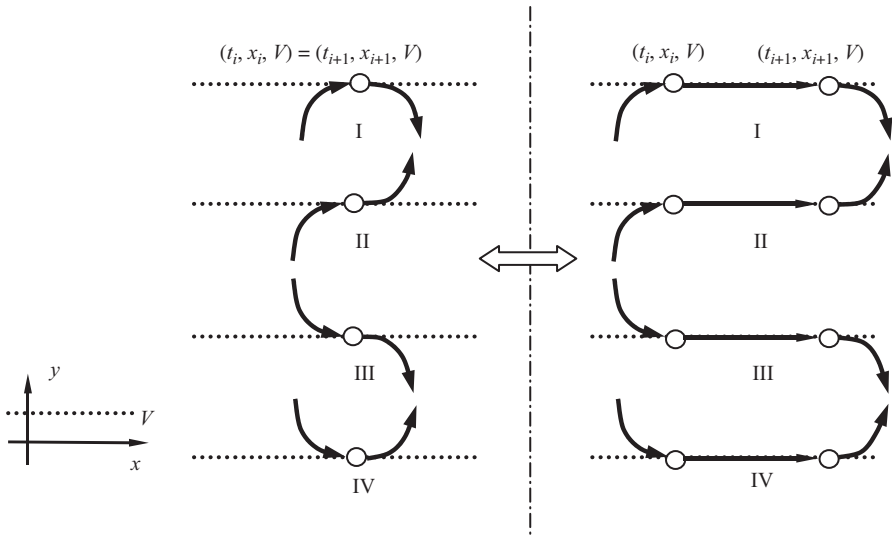

Fig. 5. The four onsets of the sliding motion and the corresponding sliding motion in phase plane for belt speed $V > 0$.

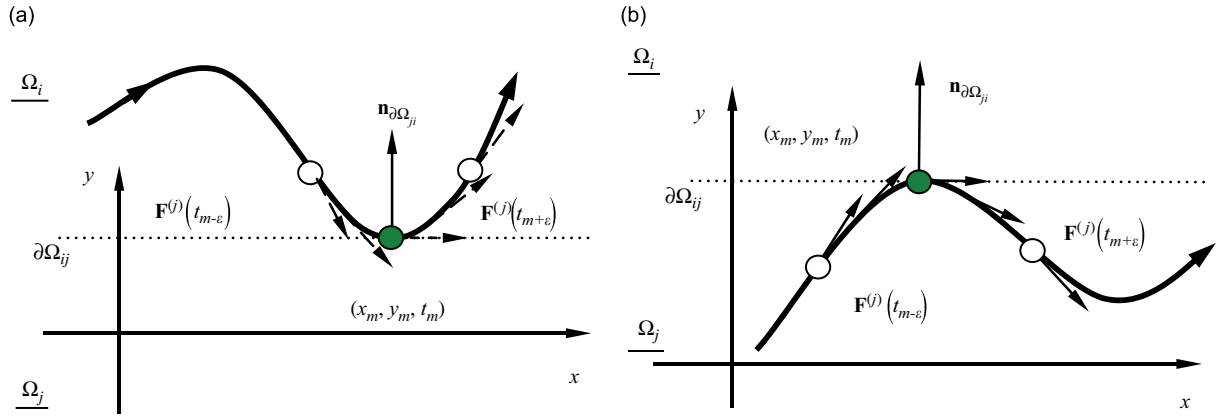

Fig. 6. Vector fields of grazing motions near the boundary $\partial\Omega_{ij}$ in (a) Ω_i and (b) Ω_j with $i,j \in \{1,2,3,4\}$.

From Luo [5], the grazing motion in Fig. 6 is guaranteed by the following conditions:

$$\begin{aligned}
&\left[\mathbf{n}^{\mathrm{T}}_{\partial\Omega_{\alpha\beta}} \cdot \mathbf{F}^{(\alpha)}(\mathbf{x}_m, t_{m\pm})\right] = 0,\ \alpha,\beta \in \{i,j\} \quad \text{and} \quad \alpha \neq \beta,\\
&\left[\mathbf{n}^{\mathrm{T}}_{\partial\Omega_{ij}} \cdot D\mathbf{F}^{(i)}(\mathbf{x}_m, t_{m\pm})\right] > 0, \quad \left[\mathbf{n}^{\mathrm{T}}_{\partial\Omega_{ij}} \cdot D\mathbf{F}^{(j)}(\mathbf{x}_m, t_{m\pm})\right] < 0 \quad \text{for} \quad \partial\Omega_{ij} \in \{\partial\Omega_{21}, \partial\Omega_{13}, \text{ and } \partial\Omega_{34}\}.
\end{aligned} \tag{20}$$

where

$$D\mathbf{F}^{(i)}(\mathbf{x},t) = \left(F_i(\mathbf{x},t), \nabla F_i(\mathbf{x},t)\cdot\mathbf{F}^{(i)}(\mathbf{x},t) + \frac{\partial F_i(\mathbf{x},t)}{\partial t}\right)^{\mathrm{T}}. \tag{21}$$

The detailed discussion of the above grazing conditions can be found in Ref. [3]. With Eqs. (15), we have

$$\begin{aligned}
\mathbf{n}^{\mathrm{T}}_{\partial\Omega_{ij}} \cdot \mathbf{F}^{(i)}(\mathbf{x},t) &= F_i(\mathbf{x},\Omega t),\\
\mathbf{n}^{\mathrm{T}}_{\partial\Omega_{ij}} \cdot D\mathbf{F}^{(i)}(\mathbf{x},t) &= \nabla F_i(\mathbf{x},\Omega t)\cdot\mathbf{F}^{(i)}(\mathbf{x},t) + \tfrac{\partial F_i(\mathbf{x},\Omega t)}{\partial t}.
\end{aligned} \tag{22}$$

From Eqs. (20) and (22), the force conditions for grazing motions in Fig. 6 are

$$\begin{aligned}
&F_\alpha(\mathbf{x}_m, \Omega t_m) = 0,\ \alpha \in \{i,j\},\\
&\nabla F_i(\mathbf{x}_m, \Omega t_{m\pm})\cdot\mathbf{F}^{(i)}(\mathbf{x}_m, t_{m\pm}) + \frac{\partial F_i(\mathbf{x}_m, \Omega t_{m\pm})}{\partial t} > 0,\\
&\nabla F_j(\mathbf{x}_m, \Omega t_{m\pm})\cdot\mathbf{F}^{(j)}(\mathbf{x}_m, t_{m\pm}) + \frac{\partial F_j(\mathbf{x}_m, \Omega t_{m\pm})}{\partial t} < 0,\\
&\quad \text{for} \quad \partial\Omega_{ij} \in \{\partial\Omega_{21}, \partial\Omega_{13}, \text{ and } \partial\Omega_{34}\}.
\end{aligned} \tag{23}$$

The kinetic friction forces on the boundaries $\partial\Omega_{34}$ and $\partial\Omega_{12}$ are C^0-continuous without the other discontinuity. It indicates the vector field in Eq. (9) is C^0-continuous. Therefore, no stick motion exists in such boundaries. Further, only the kinetic friction force was used to compute the total force. However, on $\partial\Omega_{13}$, there are the static friction forces, and once the relative motion appears, the static friction force will jump to the kinetic forces. For the non-stick motion on $\partial\Omega_{13}$, the maximum static friction force cannot be inserted, and only the kinetic friction force governs such a non-stick motion. Once the stick motion is formed on the boundary $\partial\Omega_{13}$, the maximum static friction instead of the kinetic friction one on $\partial\Omega_{13}$ governs the stick motion. For the disappearance of stick motion, the non-friction forces of the oscillator must overcome the maximum static force. Otherwise, the friction oscillator will continue to keep the stick motion on $\partial\Omega_{13}$. Thus, based on the maximum static friction force, the total forces for stick motions $\partial\Omega_{13}$ should be computed. For the stick motion on the boundary $\partial\Omega_{13}$, we have $x_m = V \times (t_m - t_i) + x_i$ from Eq. (3) for $t_m \in (t_i, t_f)$. t_i and t_f are the starting and final times for the sliding motion on the boundary $\partial\Omega_{13}$. Therefore, the total forces of the

input and output flows to the boundary $\partial\Omega_{13}$, at $(\mathbf{x}_m, t_m) \in \partial\Omega_{13}$, are defined as

$$F_j^{(\text{in})}(\mathbf{x}_m, t_{m-}) = -2d_jV - c_j[V(t_m - t_i) + x_i] + A_0 \cos \Omega t_m - a_j^{(k)}, \tag{24}$$

$$F_j^{(o)}(\mathbf{x}_m, t_{m-}) = -2d_jV - c_j[V(t_m - t_i) + x_i] + A_0 \cos \Omega t_m - a_j^{(s)}, \tag{25}$$

where $a_1^{(k)} = -a_3^{(k)} = \mu_k F_N/m$ and $a_1^{(s)} = -a_3^{(s)} = F_{f_s} \cdot F_{f_s}$ is the maximum static friction force. With the above two definitions, from Luo [6], the force criteria on the boundary $\partial\Omega_{13}$ in Eq. (17) becomes

$$\begin{aligned} &F_1^{(\text{in})}(\mathbf{x}_i, t_{i-}) \times F_3^{(\text{in})}(\mathbf{x}_i, t_{i-}) = 0 \quad \text{on} \quad \partial\Omega_{13} \text{ just for onset,} \\ &F_1^{(o)}(\mathbf{x}_m, t_{m-}) < 0 \quad \text{and} \quad F_3^{(o)}(\mathbf{x}_m, t_{m-}) > 0 \quad \text{on} \quad \partial\Omega_{13} \quad \text{before vanishing} \end{aligned} \tag{26a}$$

for the stick motion and

$$\begin{aligned} &F_1^{(\text{in})}(\mathbf{x}_m, t_{m-}) < 0 \quad \text{and} \quad F_3^{(\text{in})}(\mathbf{x}_m, t_{m+}) < 0 \quad \text{for} \quad \Omega_1 \to \Omega_3, \\ &F_1^{(\text{in})}(\mathbf{x}_m, t_{m+}) > 0 \quad \text{and} \quad F_3^{(\text{in})}(\mathbf{x}_m, t_{m-}) > 0 \quad \text{for} \quad \Omega_3 \to \Omega_1 \end{aligned} \tag{26b}$$

for the non-stick motion.

From Eq. (18), the onset conditions for the stick motion on the boundary $\partial\Omega_{13}$ are given by

$$\begin{aligned} &F_1^{(\text{in})}(\mathbf{x}_m, t_{m-}) < 0 \quad \text{and} \quad F_3^{(\text{in})}(\mathbf{x}_m, t_{m+}) = 0 \quad \text{for} \quad \Omega_1 \to \partial\Omega_{13}, \\ &F_3^{(\text{in})}(\mathbf{x}_m, t_{m-}) > 0 \quad \text{and} \quad F_1^{(\text{in})}(\mathbf{x}_m, t_{m+}) = 0 \quad \text{for} \quad \Omega_3 \to \partial\Omega_{13}. \end{aligned} \tag{27}$$

The force conditions in Eq. (19) for vanishing of the stick motion on the boundary $\partial\Omega_{13}$ become

$$\begin{aligned} &F_1^{(o)}(\mathbf{x}_m, t_{m-}) < 0 \quad \text{and} \quad F_3^{(o)}(\mathbf{x}_m, t_{m-}) = 0 \quad \text{for} \quad \partial\Omega_{13} \to \Omega_3, \\ &F_3^{(o)}(\mathbf{x}_m, t_{m-}) > 0 \quad \text{and} \quad F_1^{(o)}(x_m, t_{m-}) = 0 \quad \text{for} \quad \partial\Omega_{13} \to \Omega_1. \end{aligned} \tag{28}$$

With Eq. (24), the force conditions in Eq. (23) for grazing on $\partial\Omega_{13}$ become

$$\begin{aligned} &F_\alpha^{(\text{in})}(\mathbf{x}_m, \Omega t_m) = 0, \quad \alpha \in \{1, 3\}, \\ &\nabla F_1^{(\text{in})}(\mathbf{x}_m, \Omega t_{m\pm}) \bullet \mathbf{F}^{(1)}(\mathbf{x}_m, t_{m\pm}) + \frac{\partial F_1^{(\text{in})}(\mathbf{x}_m, \Omega t_{m\pm})}{\partial t} > 0, \\ &\nabla F_3^{(\text{in})}(\mathbf{x}_m, \Omega t_{m\pm}) \bullet \mathbf{F}^{(3)}(\mathbf{x}_m, t_{m\pm}) + \frac{\partial F_3^{(\text{in})}(\mathbf{x}_m, \Omega t_{m\pm})}{\partial t} < 0. \end{aligned} \tag{29}$$

The force conditions for grazing at the boundaries $\partial\Omega_{12}$ and $\partial\Omega_{34}$ are unchanged as in Eq. (23). From the foregoing force conditions, all the possible periodic motions for the friction oscillator in Eq. (5) can be determined.

3. Generic mappings

To determine periodic motions in such an oscillator, with an initial condition (t_i, x_i, V), the direct integration of Eq. (3) yields

$$x = V(t - t_i) + x_i. \tag{30}$$

Substitution of Eq. (24) into Eq. (11) produces the forces for a very small-neighborhood of the stick motion ($\delta \to 0$) in the domain Ω_j ($j \in \{1, 3\}$), i.e.,

$$F_j(t_{m-}) = -2d_jV - c_j[V(t_m - t_i) + x_i] + A_0 \cos \Omega t_m - a_j^{(s)} \tag{31}$$

for this problem. For non-stick motions, the initial condition on the discontinuous boundary is selected, and the coefficients of the solutions is listed in Appendices A and B, $C_k^{(j)}(x_i, \dot{x}_i, t_i) \triangleq C_k^{(j)}(x_i, t_i)$ for $k = 1, 2$. The basic solutions in Appendix A will be used for development of mappings.

In order to develop generic mappings, the discontinuous boundaries should be numbered. The boundary with the friction force jump is named by Σ_1, and the other separation boundaries are Σ_2 and Σ_3. The three

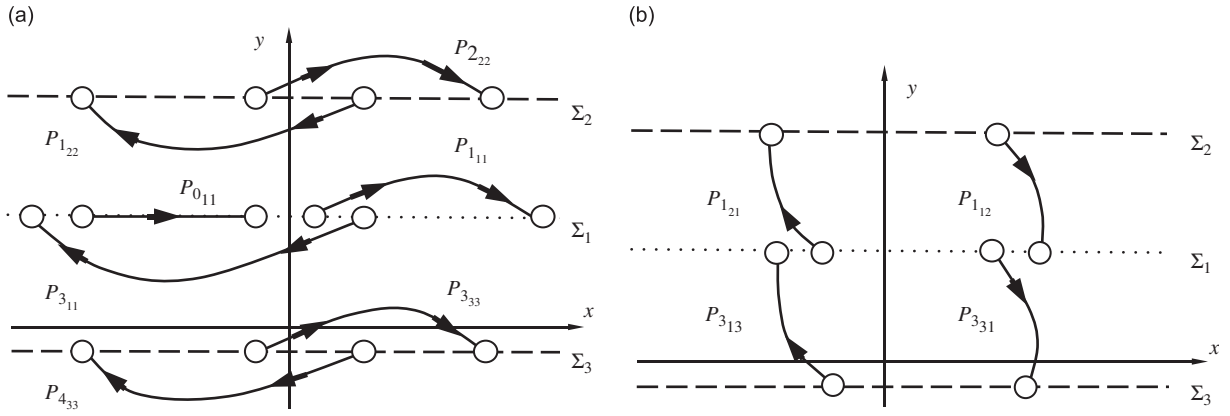

Fig. 7. Regular and stick mappings: (a) local and stick mappings and (b) global mappings.

boundaries are

$$\Sigma_\alpha = \Sigma_\alpha^0 \cup \Sigma_\alpha^+ \cup \Sigma_\alpha^- \quad \text{for} \quad \alpha = 1, 2, 3. \tag{32}$$

The corresponding, switching planes are defined as

$$\Sigma_\alpha^0 = \left\{(x_i, \Omega t_i)\middle|\dot{x}_i(t_i) = V_\rho\right\}, \quad \Sigma_\alpha^\pm = \left\{(x_i, \Omega t_i)\middle|\dot{x}_i(t_i) = V_\rho^\pm\right\}, \tag{33}$$

where $V_\sigma^\pm = \lim_{\varepsilon\to 0}(V_\sigma \pm \varepsilon)$ for an arbitrarily small $\varepsilon > 0$ and $\rho = \{\varnothing, 1, 2\}$ for $\alpha = 1, 2, 3$. In phase plane, the trajectories in Ω_j starting and ending at the separation boundaries are sketched in Fig. 7. The starting and ending points for mappings $P_{j_{\beta\alpha}}$ in Ω_j are $(x_i, \dot{x}_i, t_i)$ on Σ_α and $(x_{i+1}, \dot{x}_{i+1}, t_{i+1})$ on Σ_β, respectively. Notice that the indices $j = 1, 2, 3, 4$ and $\alpha, \beta = 1, 2, 3$ are for domains and boundaries, respectively. The stick mapping is $P_{0_{11}}$. Therefore, the mappings can be expressed through the switching sets as

$$\left.\begin{aligned} &P_{1_{11}} : \Sigma_1^+ \xrightarrow{\Omega_1} \Sigma_1^+, P_{3_{11}} : \Sigma_1^- \xrightarrow{\Omega_3} \Sigma_1^-, \\ &P_{2_{22}} : \Sigma_2^+ \xrightarrow{\Omega_2} \Sigma_2^+, P_{1_{22}} : \Sigma_2^- \xrightarrow{\Omega_1} \Sigma_2^-, \\ &P_{4_{33}} : \Sigma_3^- \xrightarrow{\Omega_4} \Sigma_3^-, P_{3_{33}} : \Sigma_3^+ \xrightarrow{\Omega_3} \Sigma_3^+; \end{aligned}\right\} \tag{34}$$

for the local mappings,

$$\left.\begin{aligned} &P_{1_{21}} : \Sigma_1^+ \xrightarrow{\Omega_1} \Sigma_2^-, \quad P_{1_{12}} : \Sigma_2^- \xrightarrow{\Omega_1} \Sigma_1^+, \\ &P_{3_{31}} : \Sigma_1^- \xrightarrow{\Omega_3} \Sigma_3^+, \quad P_{3_{13}} : \Sigma_3^+ \xrightarrow{\Omega_3} \Sigma_1^-; \end{aligned}\right\} \tag{35}$$

for the global mappings, and

$$P_{0_{11}} : \Sigma_1^0 \xrightarrow{\partial\Omega_{13}} \Sigma_1^0, \tag{36}$$

for the stick mapping.

The governing equations for $P_{0_{11}}$ and $j \in \{1, 3\}$ are

$$\begin{aligned} &-x_{i+1} + V(t_{i+1} - t_i) + x_i = 0, \\ &-2d_j V - c_j[V(t_{i+1} - t_i) + x_i] + A_0 \cos \Omega t - a_j^{(s)} = 0. \end{aligned} \tag{37}$$

From assumptions in Luo [5], the discontinuous dynamical system in Eq. (9) has three possible solutions in each domain Ω_i to make the global motion stable. Those solutions are listed in Appendix A. For non-stick motion, the governing equations of mapping $P_{j_{\beta\alpha}}$ with $j = 1, 2, 3, 4$ and $\alpha, \beta = 1, 2, 3$) are from the

displacement and velocity relations, i.e.,

$$f_1^{(j_{\beta\alpha})}(x_i, \Omega t_i, x_{i+1}, \Omega t_{i+1}) = 0,$$
$$f_2^{(j_{\beta\alpha})}(x_i, \Omega t_i, x_{i+1}, \Omega t_{i+1}) = 0. \tag{38}$$

4. Periodic motions

Once the generic mappings are developed, periodic motions in this discontinuous system can be investigated through the appropriate mapping structures. To demonstrate the procedure of determining periodic motions in this friction oscillator, consider a simple mapping first, i.e.,

$$P = P_{3_{11}} \circ P_{1_{11}} : \Sigma_1^+ \to \Sigma_1^-. \tag{39}$$

From the above relation, we have

$$\left.\begin{aligned} P_{1_{11}} &: \left(x_i, V^+, \Omega t_i\right) \to \left(x_{i+1}, V^+, \Omega t_{i+1}\right), \\ P_{3_{11}} &: (x_{i+1}, V^-, \Omega t_{i+1}) \to (x_{i+2}, V^-, \Omega t_{i+2}). \end{aligned}\right\} \tag{40}$$

Without the stick motion, $V^+ = V^- = V$ exists. The periodic motion $\mathbf{y}_{i+2} = P\mathbf{y}_i$ where $\mathbf{y}_i = (x_i, \Omega t_i)^{\mathrm{T}}$ during N-periods of excitation gives

$$x_{i+2} = x_i, \Omega t_{i+2} = \Omega t_i + 2N\pi. \tag{41}$$

With Eq. (38), Eqs. (40) and (41) gives $\mathbf{y}_i = (x_i, \Omega t_i)^{\mathrm{T}}$.

For a better understanding of periodic motions with a complicated mapping structure, consider the following mapping structure as an example:

$$P = P_{1_{12}2_{22}1_{21}0_{11}3_{13}4_{33}3_{31}} \triangleq P_{1_{12}} \circ P_{2_{22}} \circ P_{1_{21}} \circ P_{0_{11}} \circ P_{3_{13}} \circ P_{4_{33}} \circ P_{3_{31}}. \tag{42}$$

Based on the foregoing mapping structure, the periodic motion relative to $\mathbf{y}_{i+7} = P\mathbf{y}_i$ is sketched in Fig. 8. With the corresponding periodicity (i.e., $x_{i+7} = x_i$ and $\Omega t_{i+7} = \Omega t_i + 2N\pi$) similar to Eq. (41), the switching values of the periodic motion can be obtained.

Further, consider a generalized mapping structure:

$$P_{\sigma_m \ldots \sigma_2 \sigma_1} : (x_i, y_i, \Omega t_i,) \to (x_{i+m}, y_{i+m}, \Omega t_{i+m}), \tag{43}$$

where $P_{\sigma_m \ldots \sigma_2 \sigma_1} \triangleq P_{\sigma_m} \circ \cdots \circ P_{\sigma_2} \circ P_{\sigma_1}$ and P_{σ_i} $(i = 1,2,\ldots,m)$ is chosen from a generic mapping set $\{P_{j_{\beta\alpha}}, j = 1, 2, 3, 4$ and $\alpha, \beta = 1, 2, 3\}$. From the basic mappings defined in Eqs. (34)–(36), the corresponding mapping

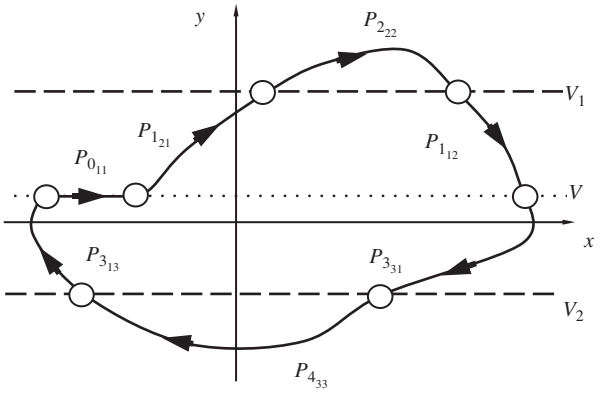

Fig. 8. Periodic motion with stick.

relations with the mapping structure $P_{\sigma_m \ldots \sigma_2 \sigma_1}$ have $2m$ equations as

$$\left.\begin{aligned} &P_{\sigma_1} : (x_i, y_i, \Omega t_i) \to (x_{i+1}, y_{i+1}, \Omega t_{i+1}),\\ &P_{\sigma_2} : (x_{i+1}, y_{i+1}, \Omega t_{i+1}) \to (x_{i+2}, y_{i+2}, \Omega t_{i+2}),\\ &\quad\vdots\\ &P_{\sigma_m} : (x_{i+m-1}, y_{i+m-1}, \Omega t_{i+m-1}) \to (x_{i+m}, y_{i+m}, \Omega t_{i+m}). \end{aligned}\right\} \tag{44}$$

The periodicity of periodic motion for the mapping structure $P_{\sigma_m \ldots \sigma_2 \sigma_1}$ gives

$$x_{i+m} = x_i, \quad \Omega t_{i+m} = \Omega t_i + 2N\pi. \tag{45}$$

Because the switching velocities $y_{i+j}\,(j = 0, 1, 2, \ldots, m)$ are given, the mapping structure with the periodicity provides the $(2m+2)$ equations required to solve the $(2m+2)$ unknowns x_{i+j} and $\Omega t_{i+j}\,(j = 0, 1, 2, \ldots, m)$. Without the stick motion, the eigenvalue analysis can provide an adequate prediction of the stability for periodic motion. The formulas for the eigenvalue analysis are presented in Appendix B. However, the eigenvalue analysis cannot work well once the stick motion is involved. Therefore, the onset, existence and disappearance of the stick motion should be determined through the force criteria in Eqs. (26)–(28). The grazing bifurcation will be determined by Eqs. (23) and (29).

Consider the system parameters: $m = 5$, $d_1 = d_2 = 0.1$, $c_1 = c_2 = 30$, $V = 3$, $V_1 = 4.5$, $V_2 = 1.5$, $\mu_s = 0.5$, $\mu_k = 0.4$, $\mu_1 = \mu_3 = 0.1$ $\mu_2 = \mu_4 = 0.5$ and $g = 9.8$ for illustrations. The switching phase and displacement varying with excitation frequency are computed for $Q_0 = 70$. The acronyms "NM" and "GB" denote the "No motion intersected with the discontinuous boundary" and "grazing bifurcation", respectively. In Fig. 9, the periodic motion with stick relative to $P_{3_{31}0_{11}3_{13}4_{33}}$ is in $\Omega \in [0.385, 3.76]$, but the non-stick periodic motion of $P_{3_{33}4_{33}}$ lies in $\Omega \in [3.76, 8.31]$. The particular values $\Omega \approx 0.385$, 3.76 and 8.31 are for grazing bifurcations. The corresponding eigenvalue analysis is completed, and the magnitudes and real parts of eigenvalues are presented in Fig. 10. The switching between two periodic motions possesses the discontinuous eigenvalues, and one of the two eigenvalues is zero for the motion with stick. It is observed that the periodic motion intersected with the discontinuous boundary disappears when two eigenvalues equal zero. For $\Omega \approx 8.31$, from two eigenvalues, the periodic motion is table. However, the grazing bifurcation occurs, no more periodic motion can be intersected with the separation boundary.

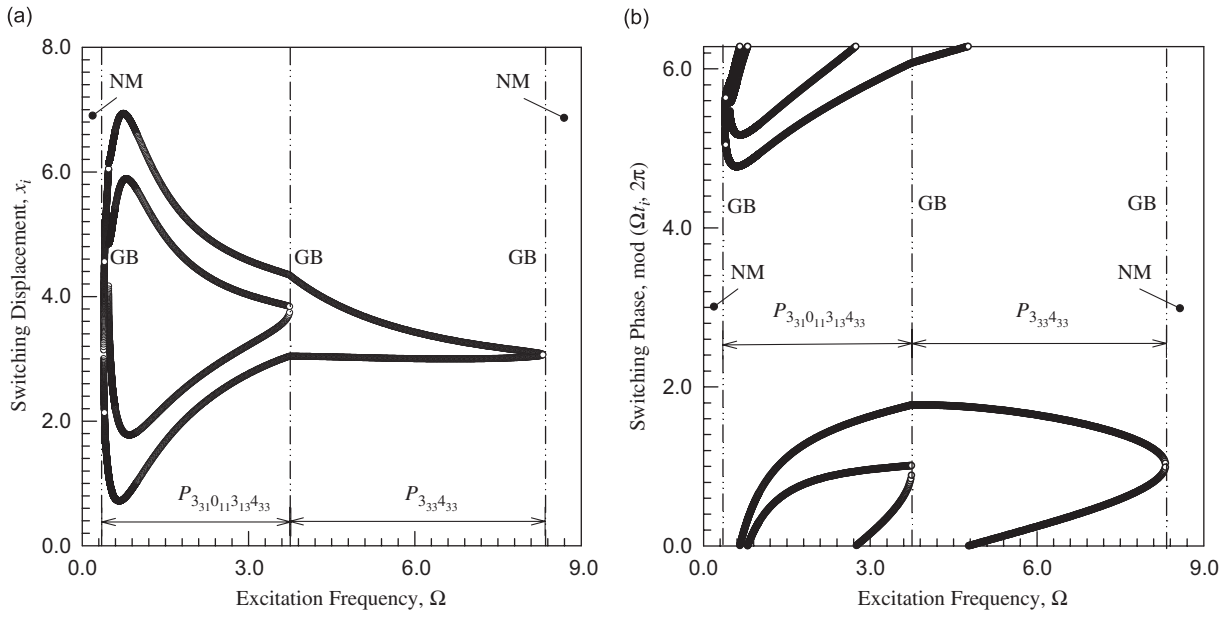

Fig. 9. (a) Switching phase and (b) switching displacement varying with excitation frequency for parameters: $m = 5$, $d_1 = d_2 = 0.1$, $c_1 = c_2 = 30$, $V = 3$, $V_1 = 4.5$, $V_2 = 1.5$, $\mu_s = 0.5$, $\mu_k = 0.4$, $\mu_1 = \mu_3 = 0.1$ $\mu_2 = \mu_4 = 0.5$ and $g = 9.8$.

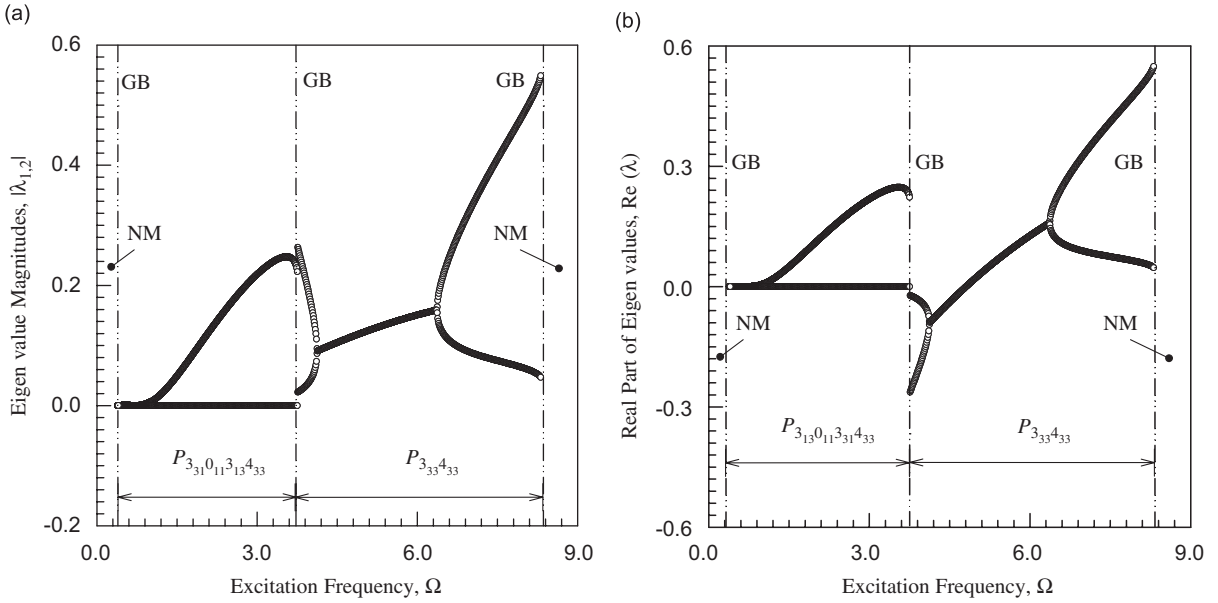

Fig. 10. (a) Magnitudes and (b) real part of eigenvalues for periodic motions varying with excitation frequency with parameters: $m = 5$, $d_1 = d_2 = 0.1$, $c_1 = c_2 = 30$, $V = 3$, $V_1 = 4.5$, $V_2 = 1.5$, $\mu_s = 0.5$, $\mu_k = 0.4$, $\mu_1 = \mu_3 = 0.1$ $\mu_2 = \mu_4 = 0.5$ and $g = 9.8$.

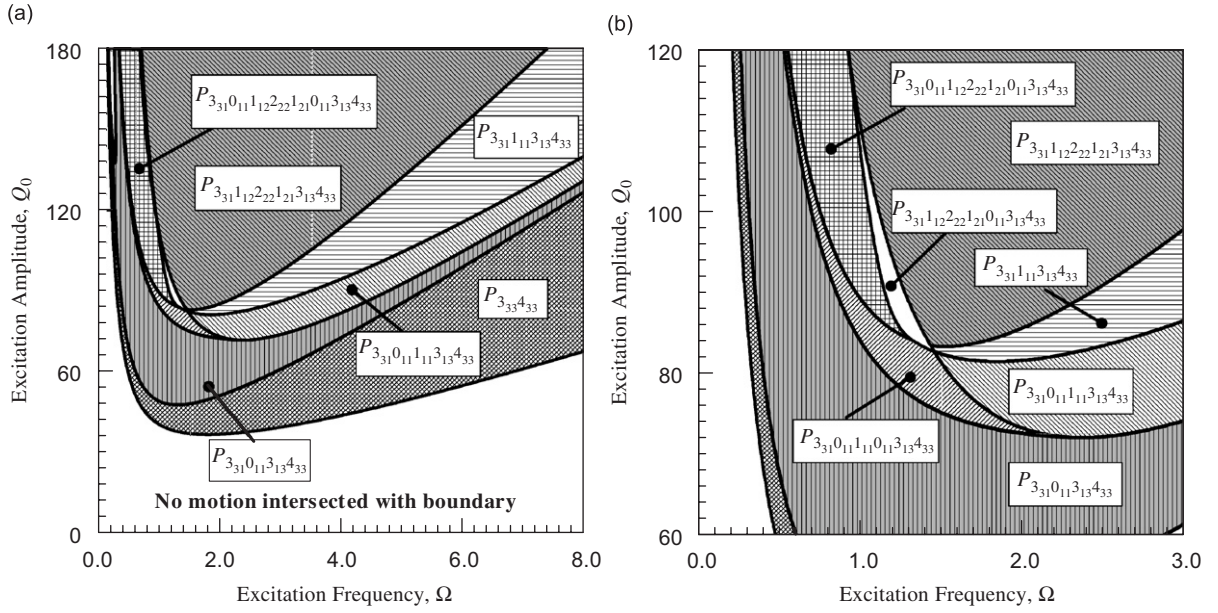

Fig. 11. Parameter map of excitation frequency and amplitude: (a) full view and (b) zoomed view. $m = 5$, $d_1 = d_2 = 0.1$, $c_1 = c_2 = 30$, $V = 3$, $V_1 = 4.5$, $V_2 = 1.5$, $\mu_s = 0.5$, $\mu_k = 0.4$, $\mu_1 = \mu_3 = 0.1$ $\mu_2 = \mu_4 = 0.5$ and $g = 9.8$.

From mapping structures, once the grazing and sliding bifurcation conditions are inserted, a parameter map between excitation frequency and amplitude is obtained and illustrated in Figs. 11(a) and (b). In Fig. 11(a), the full view of the parameter map is presented for the parameter ranges of $\Omega \in (0, 8)$ and $Q_0 \in (0, 180)$. However, in Fig. 11(b), the zoomed view of the parameter map is given for a better view of the complicated periodic

motions switching. The parameter domains relative to the corresponding mapping structures are labeled. The boundaries between the two domains are given by the sliding and grazing bifurcations. Below the domain of the periodic motion of $P_{3_{33}4_{33}}$, no any motion trajectory is intersected with the discontinuous boundary. Each domain is shaded or filled. The boundary between motions relative to $P_{3_{33}4_{33}}$ and $P_{3_{31}0_{11}3_{13}4_{33}}$ is given by the sliding bifurcation condition (or the onset of the stick motion). The boundary between periodic motions of $P_{3_{31}0_{11}3_{13}4_{33}}$ and $P_{3_{31}0_{11}1_{11}3_{13}4_{33}}$ is the onset of the passable motion on the boundary $\partial\Omega_{13}$. However, the sliding fragmentation of $P_{3_{31}0_{11}3_{13}4_{33}}$ occurs on the boundary between motions pertaining to $P_{3_{31}0_{11}3_{13}4_{33}}$ and $P_{3_{31}0_{11}1_{11}0_{11}3_{13}4_{33}}$. With varying parameters, the sliding motion from one piece becomes many pieces of the sliding and passable motions. This phenomenon is called the sliding fragmentation. The discussion of the sliding fragmentation can be referred to [4,6]. Between the periodic motions of $P_{3_{31}0_{11}1_{11}3_{13}4_{33}}$ and $P_{3_{31}0_{11}1_{11}0_{11}3_{13}4_{33}}$, a sliding bifurcation exists. The sliding motion disappearance of $P_{3_{31}0_{11}1_{11}3_{13}4_{33}}$ leads to a periodic motion pertaining to $P_{3_{31}1_{11}3_{13}4_{33}}$, and the corresponding boundary is determined by the sliding vanishing condition. From the motion of $P_{3_{31}1_{11}3_{13}4_{33}}$ to $P_{3_{31}1_{12}2_{22}1_{21}3_{13}4_{33}}$, the grazing bifurcation exists on the boundary $\partial\Omega_{12}$. In addition, from the periodic motion of $P_{3_{31}0_{11}1_{11}0_{11}3_{13}4_{33}}$ to $P_{3_{31}0_{11}1_{12}2_{22}1_{21}0_{11}3_{13}4_{33}}$, the grazing bifurcation occurs on the boundary $\partial\Omega_{12}$ again. From the periodic motion of $P_{3_{31}0_{11}1_{12}2_{22}1_{21}0_{11}3_{13}4_{33}}$ to $P_{3_{31}1_{12}2_{22}1_{21}0_{11}3_{13}4_{33}}$, the boundary for vanishing the sliding motion exists. Further, the disappearance of the sliding motion for $P_{3_{31}1_{12}2_{22}1_{21}0_{11}3_{13}4_{33}}$ produces the periodic motion relative to $P_{3_{31}1_{12}2_{22}1_{21}3_{13}4_{33}}$.

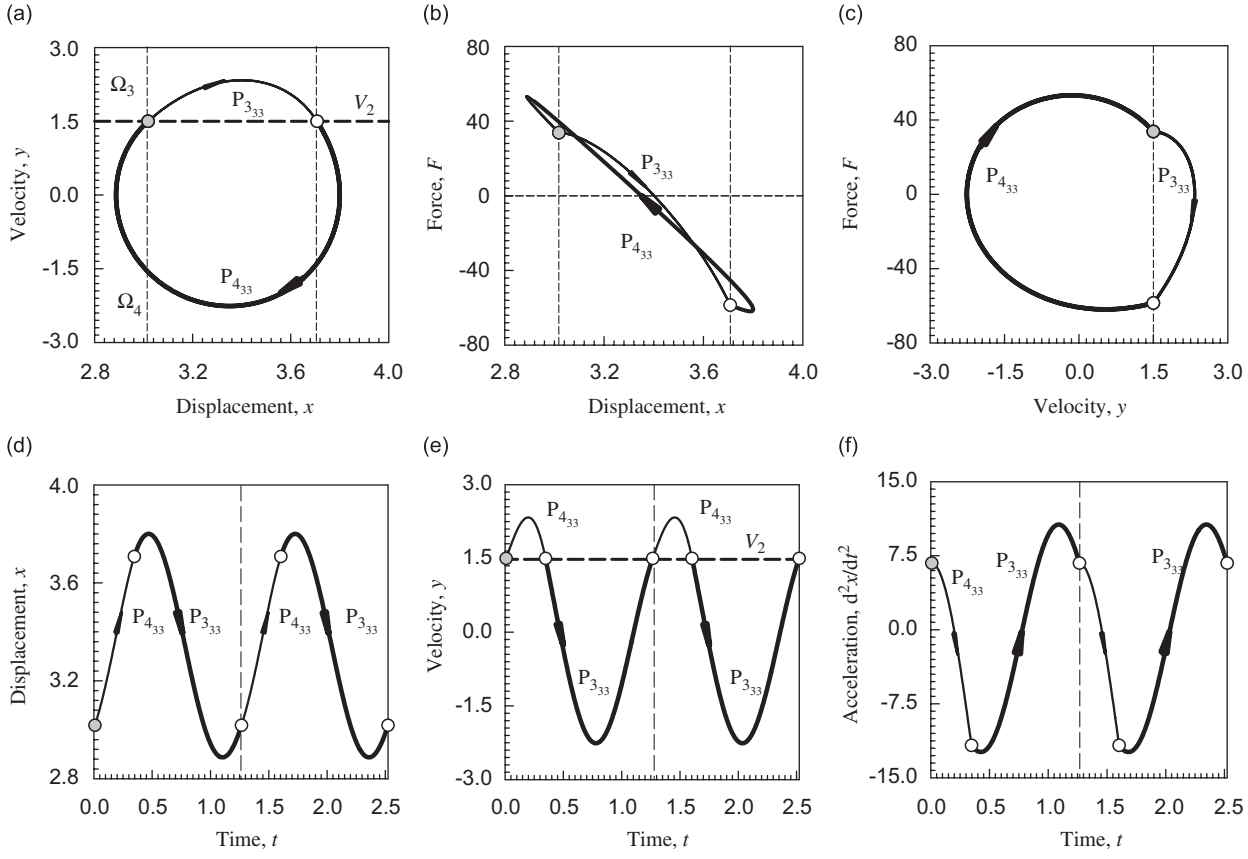

Fig. 12. Periodic responses of mapping $P_{4_{33}} \circ P_{3_{33}}$: (a) phase plane, (b) force distribution along the displacement, (c) force distribution along the velocity, (d) displacement response and (e) velocity response and (f) acceleration response for $\Omega = 5$ and $Q_0 = 70$ with the initial conditions $(\Omega t_i, x_i, \dot{x}_i) \approx (0.0458, 3.0183, 1.50)$. $m = 5$, $d_1 = d_2 = 0.1$, $c_1 = c_2 = 30$, $V = 3$, $V_1 = 4.5$, $V_2 = 1.5$, $\mu_s = 0.5$, $\mu_k = 0.4$, $\mu_1 = \mu_3 = 0.1$ $\mu_2 = \mu_4 = 0.5$ and $g = 9.8$.

5. Numerical simulations

To illustrate the analytical criteria, numerical simulations for this friction oscillator are carried out. For numerical simulations, the same parameters $m = 5$, $d_1 = d_2 = 0.1$, $c_1 = c_2 = 30$, $V = 3$, $V_1 = 4.5$, $V_2 = 1.5$, $\mu_s = 0.5$, $\mu_k = 0.4$, $\mu_1 = \mu_3 = 0.1$ $\mu_2 = \mu_4 = 0.5$ and $g = 9.8$ are used. Consider the non-stick periodic motion relative to $P_{3_{33}} \circ P_{4_{33}}$ for illustration. This periodic motion does not have the intersection with the boundary $\partial\Omega_{13}$. The periodic motion switches at the boundary $\partial\Omega_{34}$. Because the friction force on the boundary $\partial\Omega_{34}$ is C^0-continuous with the piecewise linearity in Eq. (1), the total force on the boundary $\partial\Omega_{34}$ is continuous, but the derivative of the force is discontinuous. The phase plane, force distributions along both displacement and velocity, and the responses for displacement, velocity and acceleration of the periodic motion of $P_{4_{33}3_{33}}$ are plotted in Figs. 12(a)–(f) for $\Omega = 5$ and $Q_0 = 70$ with $(\Omega t_i, x_i, \dot{x}_i) \approx (0.0458, 3.0183, 1.50)$, respectively. The responses in domains Ω_3 and Ω_4 are represented by the thin and dark curves, accordingly. The circular symbols are switching points, and the gray filled symbol is the starting point of the periodic motion. The arrow is the direction of the periodic motion. The phase plane is clearly presented in Fig. 12(a). In Figs. 12(b) and (c), it is observed that the force is not smooth at the boundary $\partial\Omega_{34}$, and the corresponding acceleration in Fig. 12(f) is not smooth as well. The displacement and velocity responses in Figs. 12(d), (e) are very smooth. In addition, the corresponding mappings are labeled on all the plots. Once the starting point is changed to another switching point, the mapping structure of the periodic motion becomes $P_{3_{33}4_{33}}$. Therefore, the two mapping structures give the same periodic motion except for the different initial conditions.

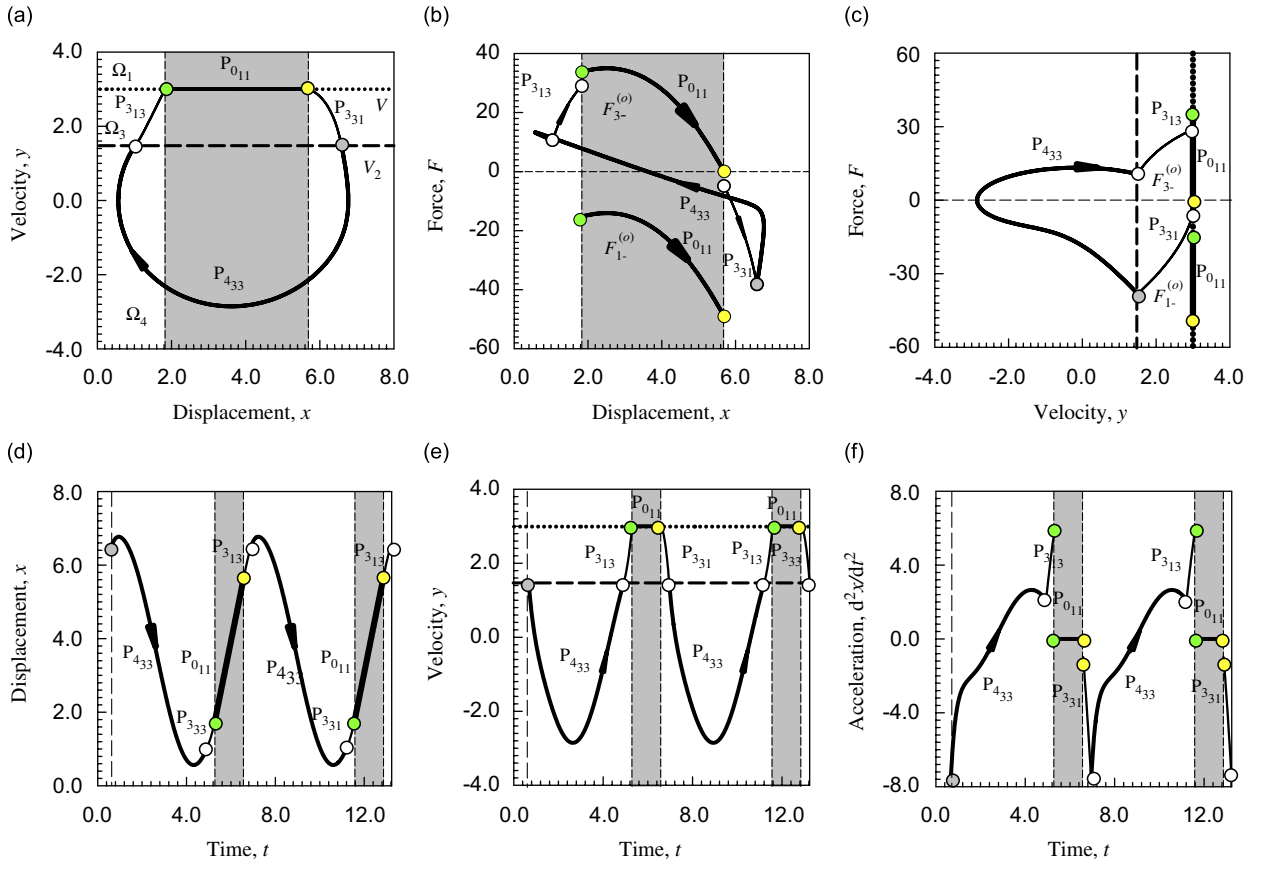

Fig. 13. Periodic responses of mapping $P_{3_{31}} \circ P_{0_{11}} \circ P_{3_{13}} \circ P_{4_{33}}$: (a) phase plane, (b) force distribution along the displacement, (c) force distribution along the velocity, (d) displacement response, (e) velocity response and (f) acceleration response for $\Omega = 1$ and $Q_0 = 70$ with the initial conditions $(\Omega t_i, x_i, \dot{x}_i) \approx (0.6672, 6.5814, 1.50)$. $m = 5$, $d_1 = d_2 = 0.1$, $c_1 = c_2 = 30$, $V = 3$, $V_1 = 4.5$, $V_2 = 1.5$, $\mu_s = 0.5$, $\mu_k = 0.4$, $\mu_1 = \mu_3 = 0.1$ $\mu_2 = \mu_4 = 0.5$ and $g = 9.8$.

Consider the second example of the stick periodic motion relative to mapping $P_{3_{31}0_{11}3_{13}4_{33}}$. The excitation frequency and amplitude $\Omega = 1$ and $Q_0 = 70$ with the initial condition $(\Omega t_i, x_i, \dot{x}_i) \approx (0.6672, 6.5814, 1.50)$ are used, and the other parameters are the same as in the first example. Again, the phase plane, force distributions along both displacement and velocity, and the responses for displacement, velocity and acceleration of the periodic motion of $P_{3_{31}0_{11}3_{13}4_{33}}$ are shown in Figs. 13(a)–(f), respectively. For this periodic motion, the sliding motion along the boundary $\partial\Omega_{13}$ exists. Because the friction force discontinuity on $\partial\Omega_{13}$ exists in Eq. (1), the discontinuity of the total force can be observed on both sides of the boundary $\partial\Omega_{13}$. In addition, the static and kinetic friction forces are different. Thus if the sticking flow wants to leave the separation boundary, the total non-friction force must overcome the static friction force. Therefore, the total force for the output flow to the boundary is defined in Eq. (25). $F^{(o)}_{\alpha-} \triangleq F^{(o)}_{\alpha}(\mathbf{x}_m, t_{m-})$ is illustrated in order to observe the force criteria for the disappearance of the stick motion. For convenience, such a total force for the output flow to the boundary is called the output flow force. The stick motion is a straight line along the discontinuous boundary in phase plane, as shown in Fig. 13(a). The force non-smoothness on the boundary $\partial\Omega_{34}$ between the two domains Ω_3 and Ω_4 is clearly observed in Fig. 13(b). If the total non-friction force is equal to or less than the kinetic friction force, the flow arriving to the boundary $\partial\Omega_{13}$ will become the stick motion. The total force for the input flow to the boundary is defined in Eq. (24), as not presented in Fig. 13(c). For convenience, the total force for the input flow to the boundary $\partial\Omega_{13}$ is called the input flow force. In Fig. 13(b), the stick motion disappears at $F^{(o)}_{3-} = 0$, it implies the non-friction force overcomes the maximum static friction force. Furthermore, the oscillator starts to oscillate on the moving belt, and the kinetic friction force should be used to estimate the total force, as in the third equation of Eq. (10) for

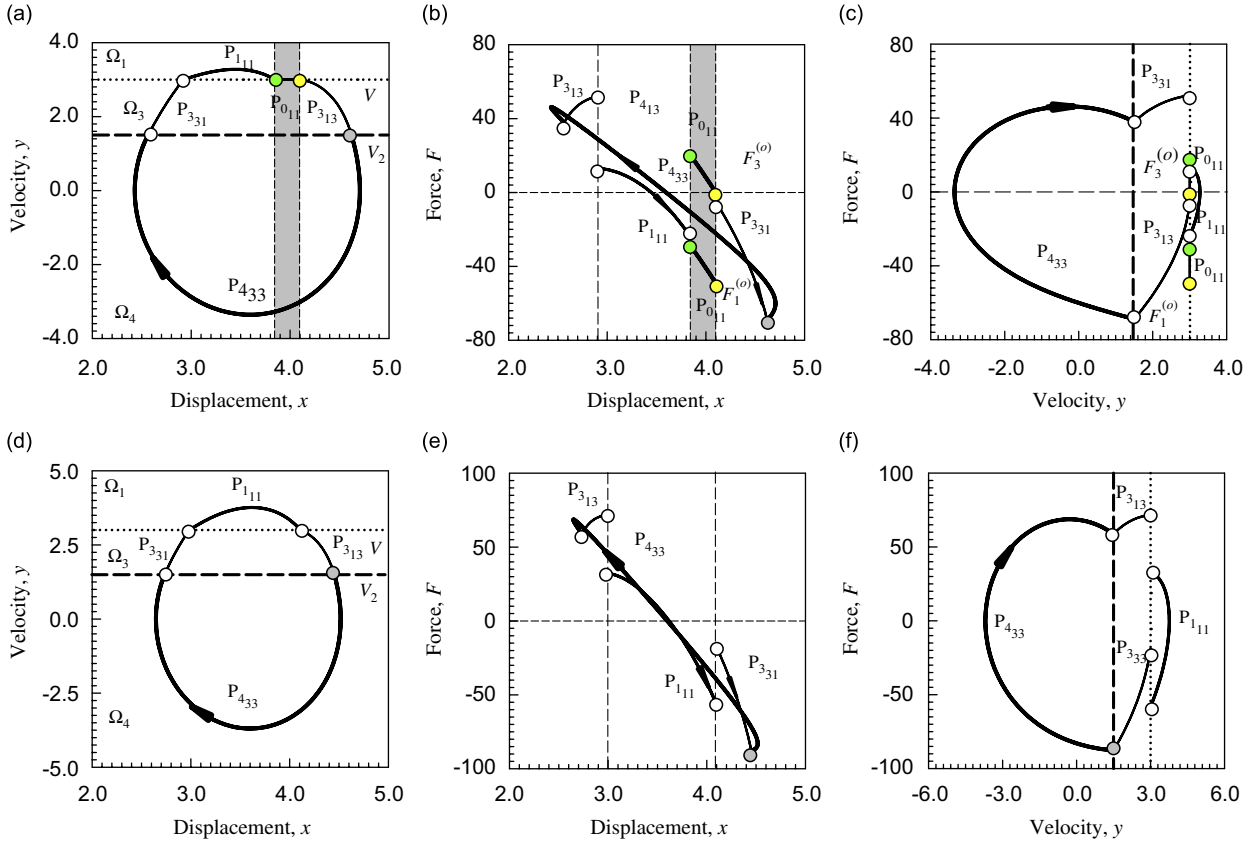

Fig. 14. Phase planes, force distributions along displacement and velocity for $V = 3$ and $x_i = 1.5$: (a)–(c) $P_{3_{31}0_{11}1_{11}3_{13}4_{33}}$ ($\Omega = 3$ and $Q_0 = 80$, $(\Omega t_i, x_i) \approx (1.6590, 4.6207)$), (d)–(f) $P_{3_{31}1_{11}3_{13}4_{33}}$ ($\Omega = 4$ and $Q_0 = 100$, $(\Omega t_i, x_i) \approx (1.8608, 4.4515)$). $m = 5$, $d_1 = d_2 = 0.1$, $c_1 = c_2 = 30$, $V = 3$, $V_1 = 4.5$, $V_2 = 1.5$, $\mu_s = 0.5$, $\mu_k = 0.4$, $\mu_1 = \mu_3 = 0.1$ $\mu_2 = \mu_4 = 0.5$ and $g = 9.8$.

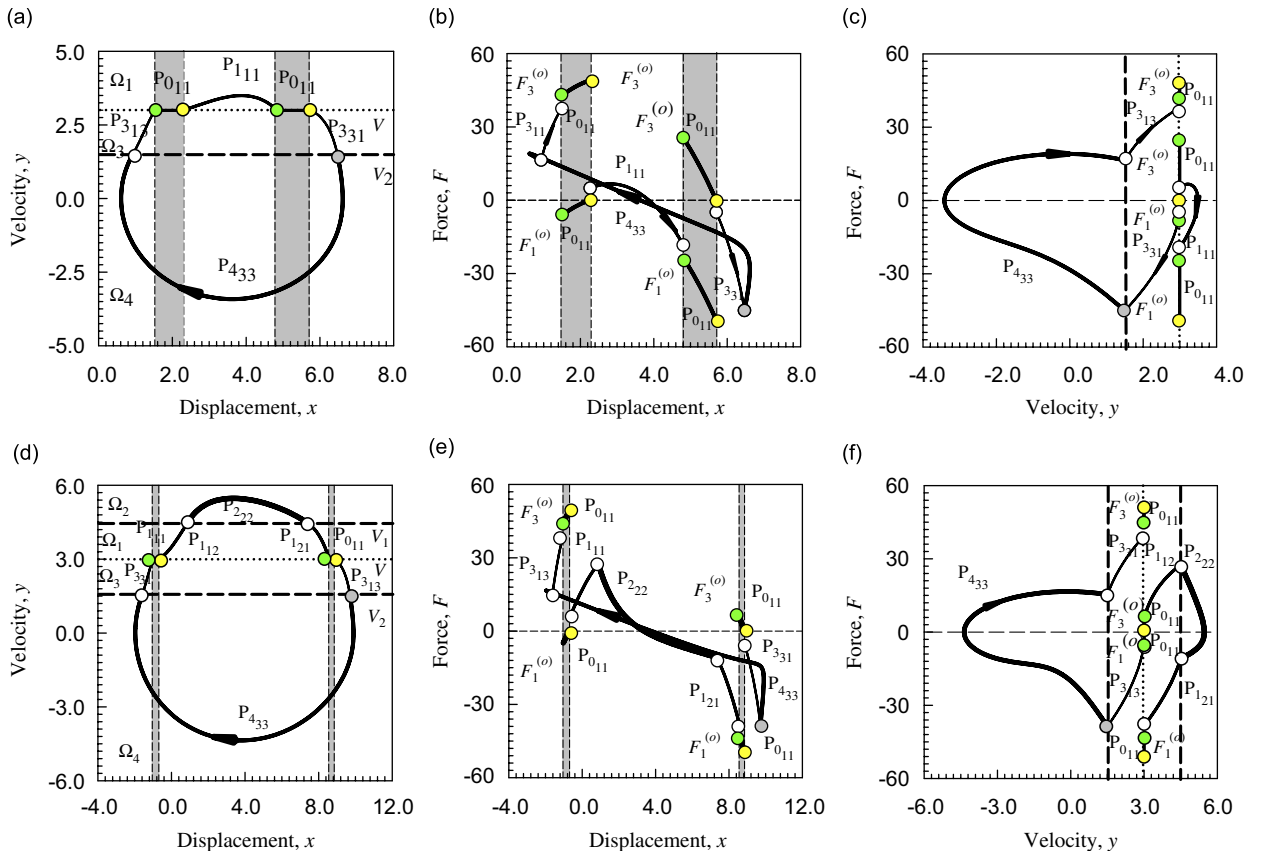

Fig. 15. Phase planes, force distributions along displacement and velocity for $V=3$ and $x_i=1.5$: (a)–(c) $P_{3_1 0_{11} 1_{11} 0_{11} 3_{13} 4_{33}}$ ($\Omega=1.2$ and $Q_0=80$, $(\Omega t_i, x_i)\approx(0.9534, 6.4731)$). (d)–(f) $P_{3_1 0_{11} 1_{12} 2_{22} 1_{21} 0_{11} 3_{13} 4_{33}}$ ($\Omega=0.8$ and $Q_0=120$, $(\Omega t_i, x_i)\approx(0.5130, 9.7127)$). $m=5$, $d_1=d_2=0.1$, $c_1=c_2=30$, $V=3$, $V_1=4.5$, $V_2=1.5$, $\mu_s=0.5$, $\mu_k=0.4$, $\mu_1=\mu_3=0.1$ $\mu_2=\mu_4=0.5$ and $g=9.8$.

motion in domain Ω_3. So the output flow force from zero jumps to the negative regular total force i.e., $F_3(\mathbf{x}, t)<0$, as observed in Fig. 13(b). Since the input flow force $F^{(o)}_{3-}>F^{(\text{in})}_{3-}>0$ and the output flow force $F^{(o)}_{1-}<0$, the stick motion appears. The non-smoothness of the forces on the boundary $\partial\Omega_{34}$ is also observed. The force characteristics of stick motion and domain switching are also presented in Fig. 13(c). From Figs. 13(d) and (e), the displacement and velocity responses are continuous. However, the acceleration is zero for the stick motion on $\partial\Omega_{13}$ and is non-smooth at $\partial\Omega_{34}$ because of the force discontinuity, which is observed in Fig. 13(f).

The phase planes and force distribution along the displacement and velocity are presented in Fig. 14(a)–(c) $P_{3_1 0_{11} 1_{11} 3_{13} 4_{33}}$ ($\Omega=3$, $Q_0=80$,$(\Omega t_i, x_i)\approx(1.6590, 4.6207)$) and (d)–(f) $P_{3_1 1_{11} 3_{13} 4_{33}}$ ($\Omega=4$ and $Q_0=100$, $(\Omega t_i, x_i)\approx(1.8608, 4.4515)$) for $V=3$ and $x_i=1.5$. When the stick motion in $P_{3_1 0_{11} 1_{11} 3_{13} 4_{33}}$ disappears, the non-stick periodic motion will exist. The periodic motion for $P_{3_1 1_{12} 2_{22} 1_{21} 0_{11} 3_{13} 4_{33}}$ ($\Omega=1.2$ and $Q_0=89$, $(\Omega t_i, x_i)\approx(0.8574, 7.2345)$) and the most complicated motion $P_{3_1 0_{11} 1_{12} 2_{22} 1_{21} 0_{11} 3_{13} 4_{33}}$ ($\Omega=0.8$ and $Q_0=120$, $(\Omega t_i, x_i)\approx(0.5130, 9.7127)$) are presented in Figs. 15(a)–(c) and (d)–(f), respectively. The complicated force distributions are given, which help one understand the necessary and sufficient conditions given in Section 2. The phase trajectories and force distributions for $P_{3_1 1_{12} 2_{22} 1_{21} 3_{13} 4_{33}}$ ($\Omega=2$, $Q_0=120$, $(\Omega t_i, x_i)\approx(1.4164, 6.9920)$) and $P_{3_1 0_{11} 1_{11} 0_{11} 3_{13} 4_{33}}$ ($\Omega=1.2$ and $Q_0=80$, $(\Omega t_i, x_i)\approx(0.9534, 6.4731)$) are also shown in Figs. 16(a)–(c) and (d)–(f), respectively. From the previous illustrations, the force criteria are very important to determine the dynamic characteristics of non-smooth dynamical systems.

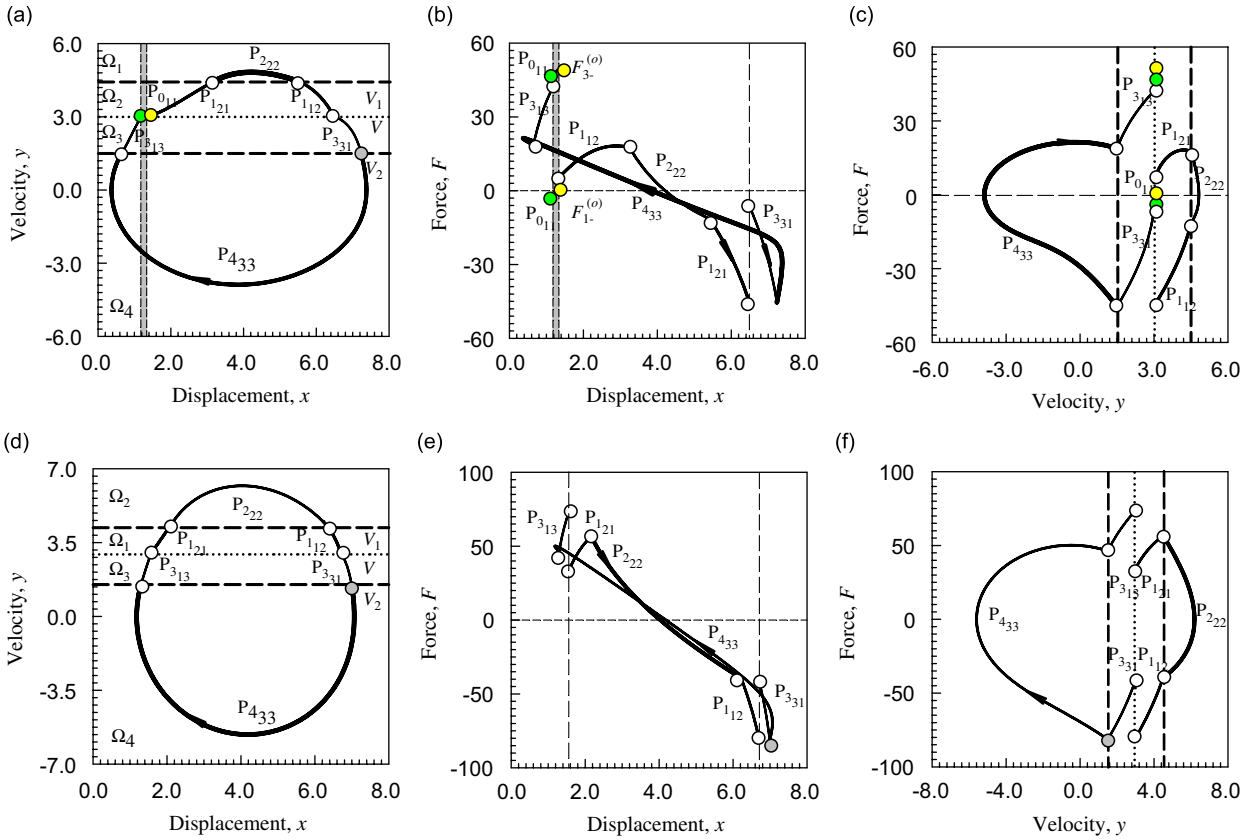

Fig. 16. Phase planes, force distributions along displacement and velocity for $V = 3$ and $x_i = 1.5$: (a)–(c) $P_{3_{31}1_{12}2_{22}1_{21}0_{11}3_{13}4_{33}}(\Omega = 1.2,\ Q_0 = 89,\ (\Omega t_i, x_i) \approx (0.8574, 7.2345)$ (d)–(f) $P_{3_{31}1_{12}2_{22}1_{21}3_{13}4_{33}}$ $(\Omega = 2,\ Q_0 = 120,\ (\Omega t_i, x_i) \approx (1.4164, 6.9920))$. $m = 5,\ d_1 = d_2 = 0.1,\ c_1 = c_2 = 30,\ V = 3,\ V_1 = 4.5,\ V_2 = 1.5,\ \mu_s = 0.5,\ \mu_k = 0.4,\ \mu_1 = \mu_3 = 0.1\ \mu_2 = \mu_4 = 0.5$ and $g = 9.8$.

6. Conclusions

A periodically forced, nonlinear friction oscillator is investigated in this paper, and the nonlinear friction force is approximated by a piecewise linear, kinetic friction model with the static force. To determine the dynamics of such an oscillator, the input and output flow forces are introduced in the vicinity of the discontinuous friction force boundary. The force criteria for the onset and vanishing of stick motions are developed through the input and output flow forces. The periodic motions of such an oscillator are analytically predicted through the corresponding mapping structures. The force responses of periodic motions agreed very well with the force criteria. If the nonlinear friction force is modeled by the several portions of piecewise linear functions, the periodically forced, nonlinear friction oscillator can be more accurately predicted. However, from the force criteria developed in this paper, the numerical prediction of the fully nonlinear friction oscillator can be carried out.

Appendix A. Basic solutions

Consider a linear oscillator in the domain Ω_j:

$$\ddot{x}^{(j)} + 2d_j\dot{x}^{(j)} + c_j x^{(j)} = -b_j + A\cos\Omega t. \tag{A.1}$$

With the initial condition $(x_i, \dot{x}_i, t_i)$, solution for Eq. (A.1) in two regions Ω_j ($j \in \{1, 2\}$) are for Case I, (i.e., $d_j^2 > c_j$):

$$x^{(j)}(t) = C_1^{(j)}(x_i, \dot{x}_i, t_i)\, e^{\lambda_1^{(j)}(t-t_i)} + C_2^{(j)}(x_i, \dot{x}_i, t_i)\, e^{\lambda_2^{(j)}(t-t_i)} + A^{(j)} \cos \Omega t + B^{(j)} \sin \Omega t + C^{(j)}, \tag{A.2}$$

$$\dot{x}^{(j)}(t) = \lambda_1^{(j)} C_1^{(j)}(x_i, \dot{x}_i, t_i)\, e^{\lambda_1^{(j)}(t-t_i)} + \lambda_2^{(j)} C_2^{(j)}(x_i, \dot{x}_i, t_i)\, e^{\lambda_2^{(j)}(t-t_i)} - A^{(j)}\Omega \sin \Omega t + B^{(j)}\Omega \cos \Omega t, \tag{A.3}$$

$$\begin{aligned}
\lambda_{1,2}^{(j)} &= -d_j \pm \sqrt{d_j^2 - c_j}, \quad \omega_d^{(j)} = \sqrt{d_j^2 - c_j}, \\
C_1^{(j)}(x_i, \dot{x}_i, t_i) &= \frac{1}{2\omega_d^{(j)}} \Big\{ -\Big[B^{(j)}\Omega + \Big(d_j + \omega_d^{(j)} \Big) A^{(j)} \Big] \cos \Omega t_i + \Big[A^{(j)}\Omega - \Big(d_j + \omega_d^{(j)} \Big) B^{(j)} \Big] \sin \Omega t_i + \dot{x}_i \\
&\quad - \Big(d_j + \omega_d^{(j)} \Big) \big(C^{(j)} - x_i \big) \Big\}, \\
C_2^{(j)}(x_i, \dot{x}_i, t_i) &= \frac{1}{2\omega_d^{(j)}} \Big\{ \Big[B^{(j)}\Omega - \Big(\omega_d^{(j)} - d_j \Big) A^{(j)} \Big] \cos \Omega t_i - \Big[\Big(\omega_d^{(j)} - d_j \Big) B^{(j)} + A^{(j)}\Omega \Big] \sin \Omega t_i \\
&\quad - \dot{x}_i + \Big(\omega_d^{(j)} - d_j \Big) \big(x_i - C^{(j)} \big) \Big\},
\end{aligned} \tag{A.4}$$

$$A^{(j)} = \frac{A_0 \big(c_j - \Omega^2 \big)}{\big(c_j - \Omega^2 \big)^2 + \big(2 d_j \Omega \big)^2}, \quad B^{(j)} = \frac{2 d_j \Omega A_0}{\big(c_j - \Omega^2 \big)^2 + \big(2 d_j \Omega \big)^2}, \quad C^{(j)} = -\frac{b_j}{c_j}. \tag{A.5}$$

For Case II (i.e., $d_j^2 < c_j$):

$$\begin{aligned}
x^{(j)}(t) &= e^{-d_j(t-t_i)} \Big[C_1^{(j)}(x_i, \dot{x}_i, t_i) \cos \omega_d^{(j)}(t - t_i) + C_1^{(j)}(x_i, \dot{x}_i, t_i) \sin \omega_d (t - t_i) \Big] \\
&\quad + A^{(j)} \cos \Omega t + B^{(j)} \sin \Omega t + C^{(j)},
\end{aligned} \tag{A.6}$$

$$\begin{aligned}
\dot{x}^{(j)}(t) &= \Big\{ \Big[\omega_d C_2^{(j)}(x_i, \dot{x}_i, t_i) - d_j C_1^{(j)}(x_i, \dot{x}_i, t_i) \Big] \cos \omega_d (t - t_i) \\
&\quad - \Big[\omega_d C_1^{(j)}(x_i, t_i) + d_j C_2^{(j)}(x_i, \dot{x}_i, t_i) \Big] \sin \omega_d (t - t_i) \Big\} e^{-d_j(t-t_i)} - A^{(j)}\Omega \sin \Omega t + B^{(j)}\Omega \cos \Omega t,
\end{aligned} \tag{A.7}$$

$$\begin{aligned}
\omega_d^{(j)} &= \sqrt{c_j - d_j^2}, \quad C_1^{(j)}(x_i, \dot{x}_i, t_i) = x_i - A^{(j)} \cos \Omega t_i - B^{(j)} \sin \Omega t_i - C^{(j)}, \\
C_2^{(j)}(x_i, \dot{x}_i, t_i) &= \frac{1}{\omega_d^{(j)}} \big[\dot{x}_i - \big(d_j A + B\Omega \big) \cos \Omega t_i - \big(d_j B^{(j)} - A^{(j)}\Omega \big) \sin \Omega t_i + d_j \big(x_i - C^{(j)} \big) \big].
\end{aligned} \tag{A.8}$$

For Case III (i.e., $d_j^2 = c_j$):

$$x^{(j)}(t) = \Big[C_1^{(j)}(x_i, \dot{x}_i, t_i) + C_2^{(j)}(x_i, \dot{x}_i, t_i) \times (t - t_i) \Big] e^{\lambda_1^{(j)}(t-t_i)} + A^{(j)} \cos \Omega t + B^{(j)} \sin \Omega t + C^{(j)}, \tag{A.9}$$

$$\begin{aligned}
\dot{x}^{(j)}(t) &= \Big[\lambda_1^{(j)} C_1^{(j)}(x_i, \dot{x}_i, t_i) + C_2^{(j)}(x_i, \dot{x}_i, t_i) \Big] e^{\lambda_1^{(j)}(t-t_i)} + \lambda_1^{(j)} C_2^{(j)}(x_i, \dot{x}_i, t_i) \times (t - t_i)\, e^{\lambda_1^{(j)}(t-t_i)} \\
&\quad - A^{(j)}\Omega \sin \Omega t + B^{(j)}\Omega \cos \Omega t,
\end{aligned} \tag{A.10}$$

$$\lambda_1^{(j)} = -2d_j, \quad C_1^{(j)}(x_i, \dot{x}_i, t_i) = x_i - A^{(j)} \cos \Omega t_i - B^{(j)} \sin \Omega t_i - C^{(j)},$$
$$C_2^{(j)}(x_i, \dot{x}_i, t_i) = \dot{x}_i + \left(A^{(j)}\Omega - d_j B^{(j)}\right) \sin \Omega t_i - \left(d_j A^{(j)} + B^{(j)}\Omega\right) \cos \Omega t_i - d_j\left(C^{(j)} - x_i\right). \tag{A.11}$$

Appendix B. Local stability and bifurcation

The local stability and bifurcation for periodic motion $\mathbf{y}_{i+m} = P\mathbf{y}_i$ can be determined by the eigenvalue analysis based on the Jacobian matrix:

$$\mathrm{DP} = \left[\frac{\partial(t_{i+m}, x_{i+m})}{\partial(t_i, x_i)}\right]_{(t_i, y_i)} = \prod_{j=1}^{m} \mathrm{DP}_{\sigma_j}, \tag{B.1}$$

where

$$\mathrm{DP}_{\sigma_j} = \begin{bmatrix} \dfrac{\partial t_{i+j}}{\partial t_{i+j-1}} & \dfrac{\partial t_{i+j}}{\partial x_{i+j-1}} \\ \dfrac{\partial x_{i+j}}{\partial t_{i+j-1}} & \dfrac{\partial x_{i+j}}{\partial x_{i+j-1}} \end{bmatrix} \tag{B.2}$$

and the matrix components $\partial t_{i+j}/\partial t_{i+j-1}$, $\partial t_{i+j}/\partial x_{i+j-1}$, $\partial x_{i+j}/\partial t_{i+j-1}$ and $\partial x_{i+j}/\partial x_{i+j-1}$ are determined through Eqs. (38) and (48). If the eigenvalues for the mapping structure of periodic motion are $\lambda_{1,2}$. The stable period-1 motion requires the eigenvalues be $|\lambda_\alpha| < 1$, ($\alpha \in \{1, 2\}$). Once the foregoing condition is not satisfied, the period-1 motion is unstable. If $|\lambda_{1 \text{ or } 2}| = 1$ with complex numbers, the Neimark bifurcation occurs. If one of the two eigenvalues is -1 (i.e., $\lambda_{(1 \text{ or } 2)} = -1$) and the other one is inside the unit circle, the period-doubling bifurcation occurs, i.e.,

$$\det(\mathrm{DP}) + \mathrm{Tr}(\mathrm{DP}) + 1 = 0, \tag{B.3}$$

where $\det(\cdot)$ and $\mathrm{Tr}(\cdot)$ are the determinant and trace of the matrix, respectively. If one of the two eigenvalues is $+1$ (i.e., $\lambda_{(1 \text{ or } 2)} = +1$) and the second one is inside the unit circle, the first saddle-node bifurcation occurs, i.e.,

$$\det(\mathrm{DP}) + 1 = \mathrm{Tr}(\mathrm{DP}). \tag{B.4}$$

References

[1] A.C.J. Luo, B.C. Gegg, On the mechanism of stick and non-stick periodic motion in a forced oscillator with dry-friction, *Journal of Vibration and Acoustics—Transactions of the ASME* 128 (2005) 97–105.
[2] A.C.J. Luo, B.C. Gegg, Stick and non-stick periodic motions in a periodically forced oscillator with dry-friction, *Journal of Sound and Vibration* 291 (2005) 132–168.
[3] A.C.J. Luo, B.C. Gegg, Grazing phenomena in a periodically forced, friction-induced, linear oscillator, *Communications in Nonlinear Science and Numerical Simulation* 11 (2006) 777–802.
[4] A.C.J. Luo, B.C. Gegg, Force product criteria of the sliding motions in a periodically forced, linear oscillator including dry friction, *Proceedings of IDETC 2005, 2005 ASME International Design Engineering Conferences and Computer and Information Conferences in Engineering*, Long Beach, California, DETC2005-84147, September 24–28, 2005.
[5] A.C.J. Luo, A theory for non-smooth dynamical systems on connectable domains, *Communications in Nonlinear Science and Numerical Simulation* 10 (2005) 1–55.
[6] A.C.J. Luo, *Singularity and Dynamics on Discontinuous Vector Fields*, Elsevier, Amsterdam, 2006.
[7] J.P. Den Hartog, Forced vibrations with Coulomb and viscous damping, *Transactions of the American Society of Mechanical Engineers* 53 (1931) 107–115.
[8] E.S. Levitan, Forced oscillation of a spring–mass system having combined Coulomb and viscous damping, *Journal of the Acoustical Society of America* 32 (1960) 1265–1269.
[9] A.F. Filippov, Differential equations with discontinuous right-hand side, *American Mathematical Society Translations, Series 2* 42 (1964) 199–231.
[10] A.F. Filippov, *Differential Equations with Discontinuous Righthand Sides*, Kluwer Academic Publishers, Dordrecht, 1988.

[11] A.C.J. Luo, Imaginary, sink and source flows in the vicinity of the separatrix of non-smooth dynamic system, *Journal of Sound and Vibration* 285 (2004) 443–456.
[12] M.S. Hundal, Response of a base excited system with Coulomb and viscous friction, *Journal of Sound and Vibration* 64 (1979) 371–378.
[13] S.W. Shaw, On the dynamic response of a system with dry-friction, *Journal of Sound and Vibration* 108 (1986) 305–325.
[14] B.F. Feeny, A non-smooth Coulomb friction oscillator, *Physica D* 59 (1992) 25–38.
[15] B.F. Feeny, F.C. Moon, Chaos in a forced dry-friction oscillator: experiments and numerical modeling, *Journal of Sound and Vibration* 170 (1994) 303–323.
[16] B.F. Feeny, The nonlinear dynamics of oscillators with stick–slip friction, in: A. Guran, F. Pfeiffer, K. Popp (Eds.), *Dynamics with Friction*, World Scientific, River Edge, 1996, pp. 36–92.
[17] N. Hinrichs, M. Oestreich, K. Popp, Dynamics of oscillators with impact and friction, *Chaos, Solitons and Fractals* 8 (4) (1997) 535–558.
[18] N. Hinrichs, M. Oestreich, K. Popp, On the modeling of friction oscillators, *Journal of Sound and Vibration* 216 (3) (1998) 435–459.
[19] S. Natsiavas, Stability of piecewise linear oscillators with viscous and dry friction damping, *Journal of Sound and Vibration* 217 (1998) 507–522.
[20] R.I. Leine, D.H. Van Campen, A. De Kraker, L. Van Den Steen, Stick–slip vibrations induced by alternate friction models, *Nonlinear Dynamics* 16 (1998) 41–54.
[21] L.N. Virgin, C.J. Begley, Grazing bifurcation and basins of attraction in an impact-friction oscillator, *Physica D* 130 (1999) 43–57.
[22] P.L. Ko, M.-C. Taponat, R. Pfaifer, Friction-induced vibration—with and without external disturbance, *Tribology International* 34 (2001) 7–24.
[23] U. Andreaus, P. Casini, Friction oscillator excited by moving base and colliding with a rigid or deformable obstacle, *International Journal of Non-linear Mechanics* 37 (2002) 117–133.
[24] J.J. Thomsen, A. Fidlin, Analytical approximations for stick–slip vibration amplitudes, *International Journal of Non-linear Mechanics* 38 (2003) 389–403.
[25] W.J. Kim, N.C. Perkins, Harmonic balance/Galerkin method for non-smooth dynamical system, *Journal of Sound and Vibration* 261 (2003) 213–224.
[26] V.N. Pilipchuk, C.A. Tan, Creep-slip capture as a possible source of squeal during decelerating sliding, *Nonlinear Dynamics* 35 (2004) 258–285.
[27] Y. Li, Z.C. Feng, Bifurcation and chaos in friction-induced vibration, *Communications in Nonlinear Science and Numerical Simulation* 9 (2004) 633–647.
[28] A.C.J. Luo, Analytical Modeling of Bifurcations, Chaos and Fractals in Nonlinear Dynamics, PhD Dissertation, University of Manitoba, Winnipeg, Canada, 1995.
[29] R.P.S. Han, A.C.J. Luo, W. Deng, Chaotic motion of a horizontal impact pair, *Journal of Sound and Vibration* 181 (1995) 231–250.
[30] A.C.J. Luo, An unsymmetrical motion in a horizontal impact oscillator, *Journal of Vibrations and Acoustics—Transactions of the ASME* 124 (2002) 420–426.
[31] S. Menon, A.C.J. Luo, An analytical prediction of the global period-1 motion in a periodically forced, piecewise linear system, *International Journal of Bifurcation and Chaos* 15 (6) (2005) 1945–1957.
[32] A.C.J. Luo, S. Menon, Global chaos in a periodically forced, linear system with a dead-zone restoring force, *Chaos, Solitons and Fractals* 19 (2004) 1189–1199.
[33] A.C.J. Luo, The mapping dynamics of periodic motions for a three-piecewise linear system under a periodic excitation, *Journal of Sound and Vibration* 283 (2005) 723–748.
[34] F. Pfeiffer, Unsteady processes in machines, *Chaos* 4 (1994) 693–705.
[35] F. Pfeiffer, Chr. Glocker, *Multibody Dynamics with Unilateral Contacts*, Wiley Series in Nonlinear Science, New York, 1996.
[36] F. Pfeiffer, Unilateral multibody dynamics, *Meccanica* 34 (2000) 437–451.
[37] F. Pfeiffer, Applications of unilateral multibody dynamics, *Philosophical Transactions Royal Society of London A* 359 (2001) 2609–2628.
[38] M. di Bernardo, P. Kowalczyk, A. Nordmark, Classification of sliding bifurcation in dry-friction oscillators, *International Journal of Bifurcation and Chaos* 13 (10) (2003) 2935–2948.
[39] U. Galvanetto, Sliding bifurcation in the dynamics of mechanical systems with dry-friction-remarks for engineers and applied scientists, *Journal of Sound and Vibration* 276 (2004) 121–139.
[40] H. Dankowicz, A.B. Nordmark, On the origin and bifurcations of stick–slip oscillations, *Physica D* 136 (2000) 280–302.